Ecole de Physique des Astroparticules, OHP, 7-12 septembre 2009

Measurements of cosmic ray fluxes with PAMELA apparatus

Sergio Ricciarini
INFN – Florence, Italy

On behalf of the PAMELA collaboration

Summary

- **This presentation is aimed at understanding experimental and data analysis issues of PAMELA measurements.**
- **(1) The PAMELA experiment:**
  - **description of mission and apparatus; principle of operation.**
- **(2) Measurement of relative fluxes of antiparticles:**
  - **(2.a) antiproton/proton ratio;**
  - **(2.b) positron/(positron+electron).**
- **(3) Measurement of absolute fluxes:**
  - **(3.a) protons;**
  - **(3.b) antiprotons;**
  - **(3.c) Helium;**
  - **(3.d) electrons.**

(1) The PAMELA experiment

The PAMELA collaboration

Italy

INFN

Bari

Florence

Naples

Rome

Trieste

Frascati

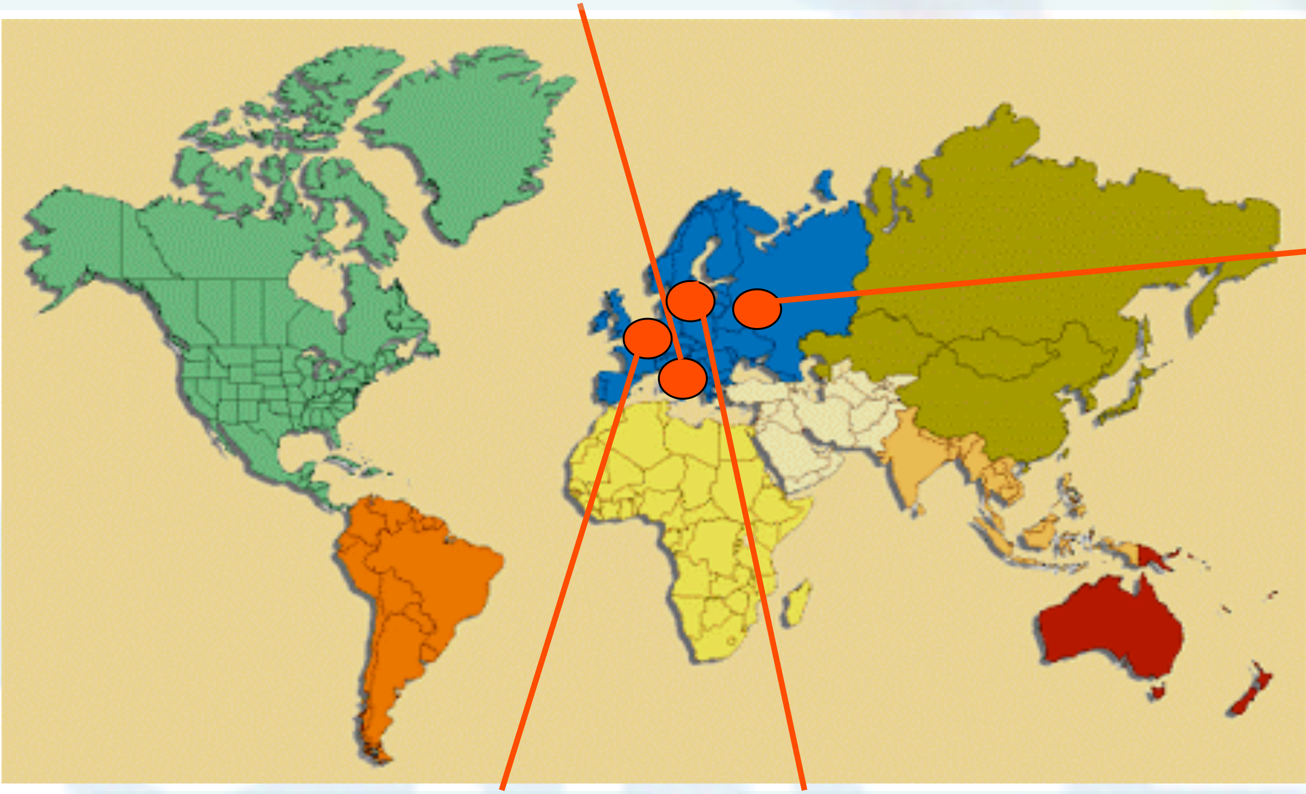

Russia

Moscow,
St. Petersburg

Germany

Siegen

Sweden

Stockholm

PAMELA scientific objectives

- **Study antiparticles in cosmic rays.**
- **Search for dark matter annihilation (e^+ and p-bar spectra).**
- **Study cosmic-ray production and propagation.**
- **Study composition and spectra of cosmic rays (including light nuclei).**
- **Search for anti-He (primordial antimatter).**
- **Study solar physics and solar modulation.**
- **Study of terrestrial magnetosphere and radiation belts.**

The mission

- **PAMELA installed on Russian satellite Resurs-DK1, inside a pressurized container.**
  - **Mission started on June 2006, extended to 5 years total lifetime.**

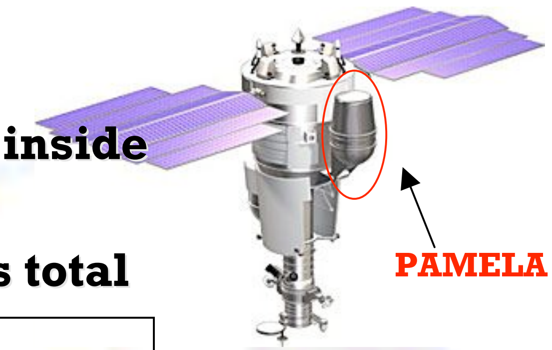

Quasi-polar low-earth elliptical orbit (70.0°, 350 - 610 km).

- Traverses and operates in the South Atlantic Anomaly.

- Crosses the outer (electron) Van Allen belt at south pole.

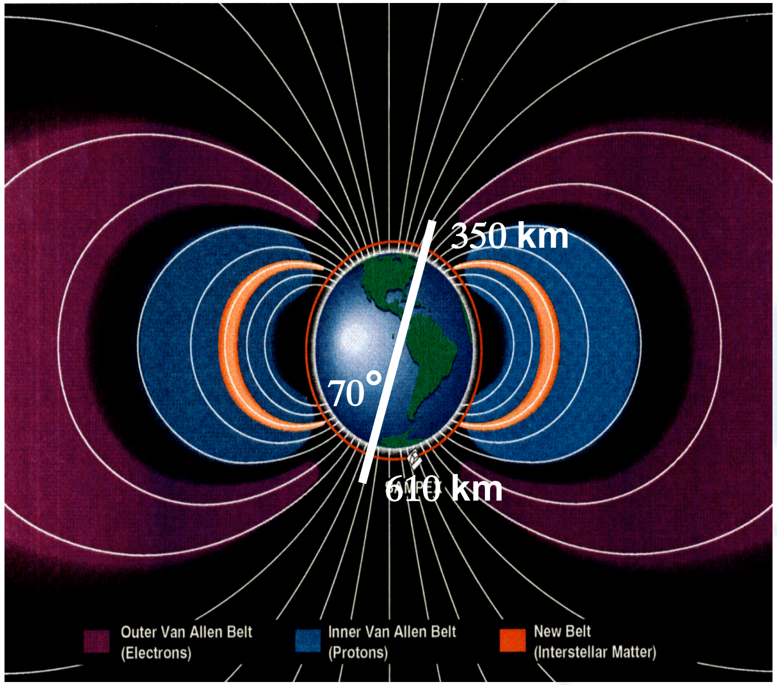

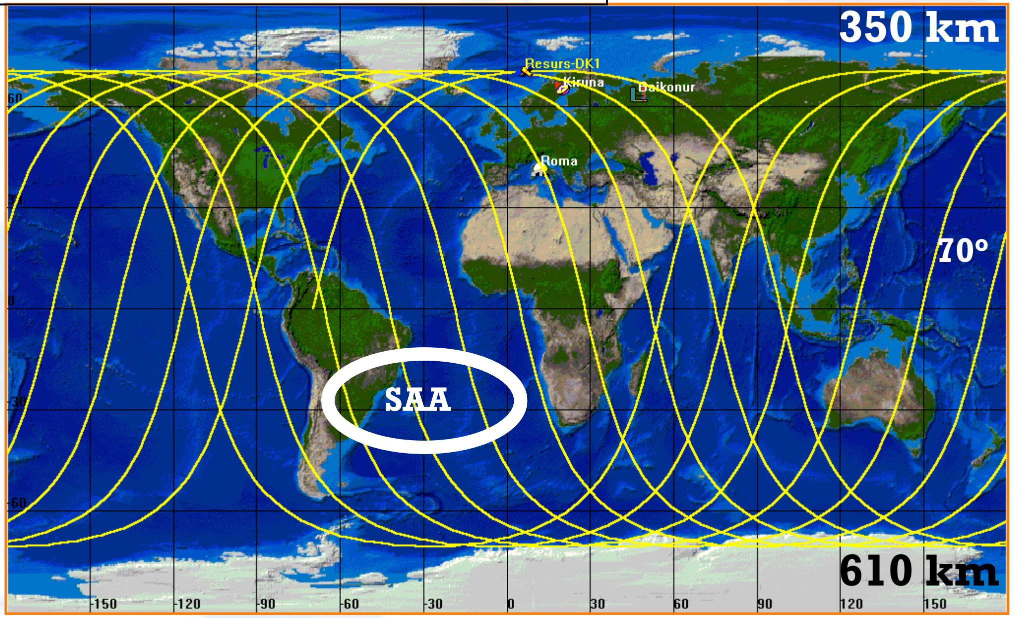

orbit period ~90 min

Trigger rate

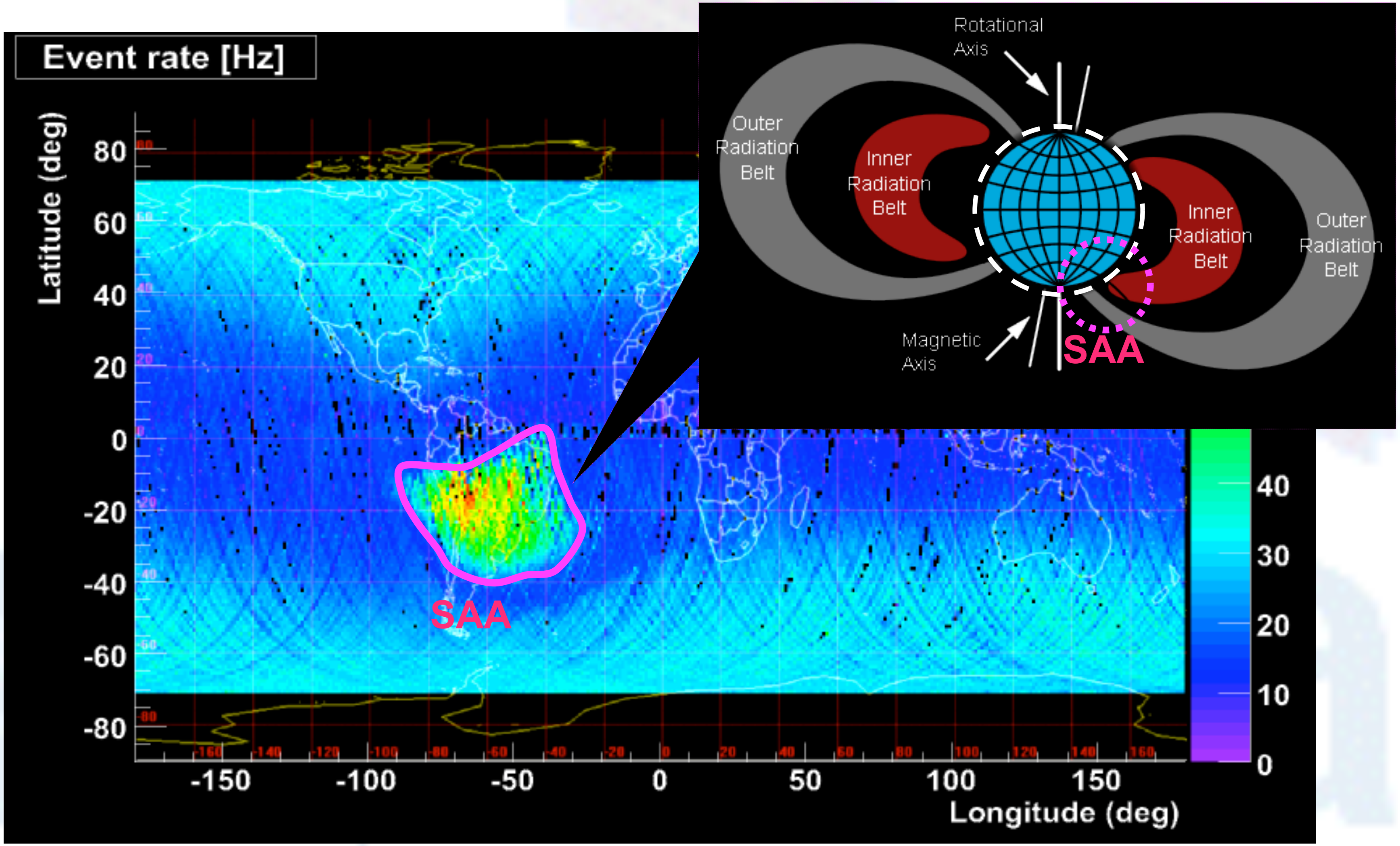

The instrument

Main requirements: high-sensitivity particle identification and precise momentum measurement

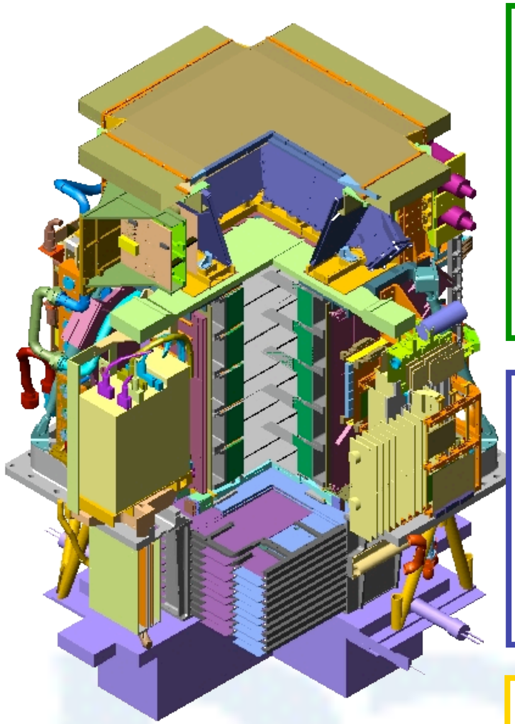

GF: 21.6 cm² sr
Mass: 470 kg
Size: 130 · 70 · 70 cm³
Power Budget: 360 W

Time-Of-Flight (TOF)
plastic scintillators + PMT:
- Trigger
- Upward-going rejection
- Mass identification up to 1 GeV
- Charge value from dE/dL

Electromagnetic calorimeter
W/Si sampling (16.3 X_0, 0.6 λ_I)
- Discrimination e^+ / p, p-bar / e^- (shower topology)
- Direct E measurement for e^-/e^+

Neutron detector
polyethylene + ^{3}He counters:
- High-energy e/h discrimination

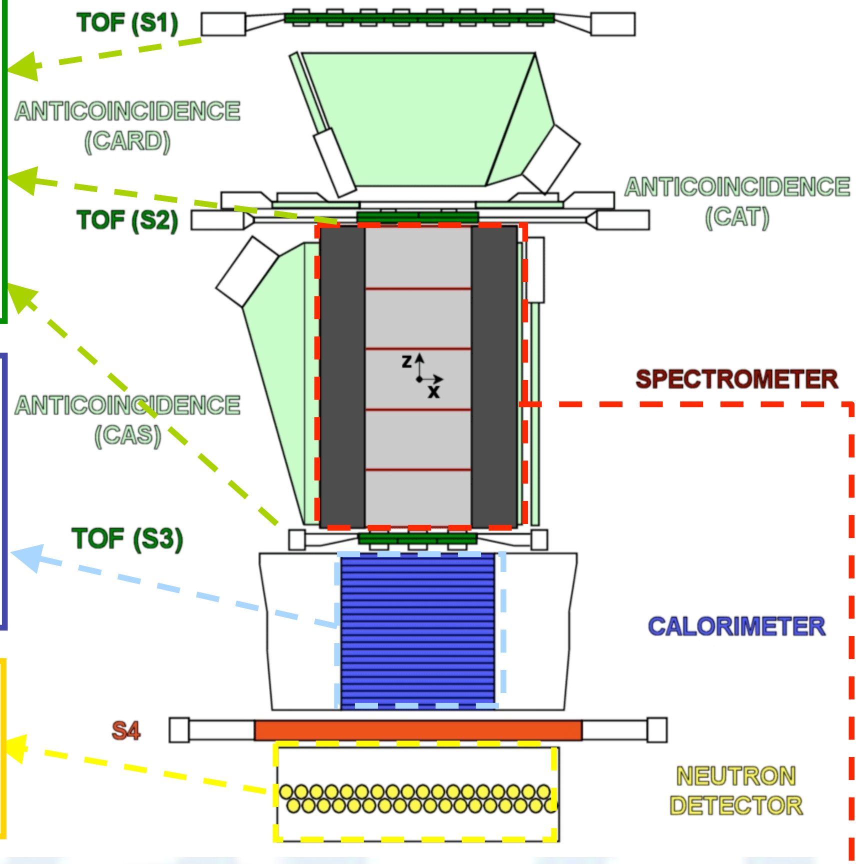

Spectrometer
microstrip Si tracking system (TRK) + permanent magnet
- Charge sign (particle/antiparticle discrimination)
- Momentum
- Charge value from dE/dL

Track reconstruction

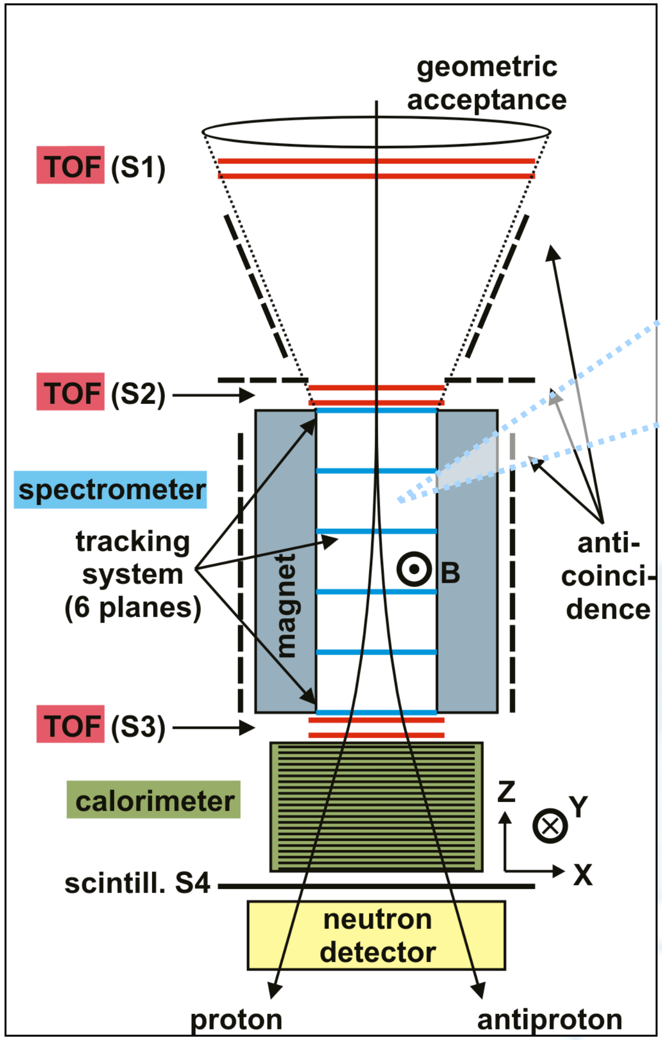

Magnetic spectrometer

- permanent hollow magnet.
- 6 planes of double-sided (X-Y) microstrip Si sensors.
- Spatial resolution: 3÷4 mm.

- Iterative χ^2 minimization as a function of track state-vector components α.

$\alpha = (x_0, y_0, \sin\theta, \phi, \eta)$

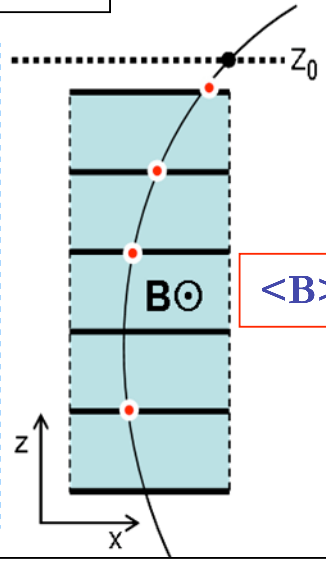

$\langle B \rangle = 0.43$ T

Magnetic rigidity: $R = pc/Ze$ (**GV**)
(includes sign of the charge Z)

Magnetic deflection: $\eta = 1/R$ (GV^{-1})

MDR (Maximum Detectable Rigidity)
value of |R| for which $\sigma_R = |R|$

MDR ~ 1 TV

(σ_R directly measured at beam test)

In-flight spectrometer alignment (1/2)

- **Step 1: incoherent alignment.**
  - **correction for random displacements of the sensors (~ 10 μm);**
  - **done with relativistic protons;**
  - **minimization of spatial residuals as a function of the roto-traslational parameters of each sensor.**

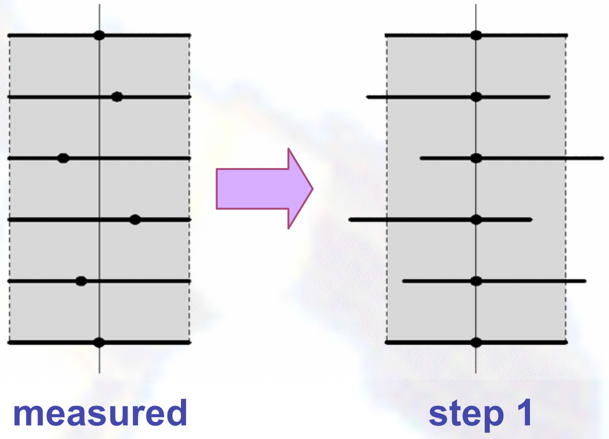

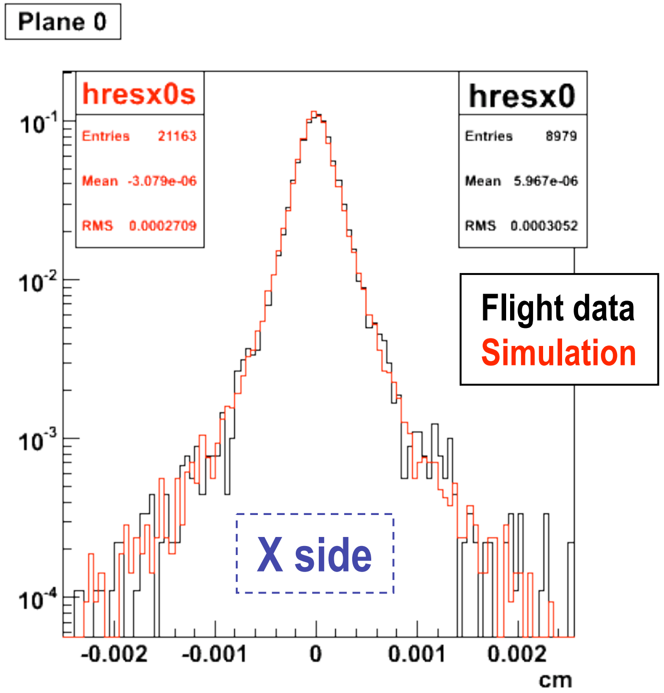

- **After step 1:**
  - **spatial residuals are centered;**
  - **measured width is consistent with simulated combination of nominal resolution + alignment uncertainty (~ 1 μm).**

In-flight spectrometer alignment (2/2)

- **After step 1, (possible) global distortions might mimic a residual deflection: $\eta_{meas} = \eta_{real} + \Delta\eta$.**

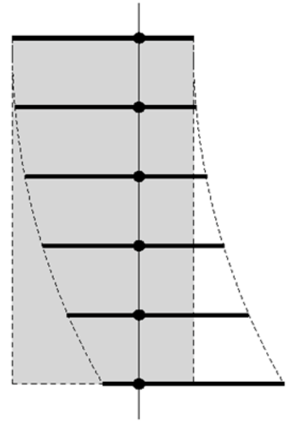

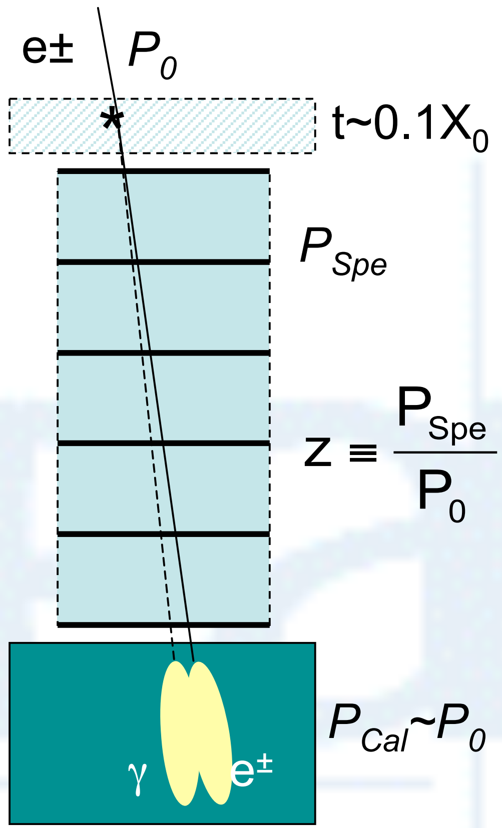

- **Step 2: coherent alignment.**
  - **done with electrons and positrons;**
  - **cross-calibration CALO-TRK exploiting brehmsstrahlung before spectrometer:**

$$z \sim \frac{1}{P_{Cal} \cdot |\eta_{Spe}|} \longrightarrow \frac{1}{P_{Cal}(1 \pm \varepsilon) \cdot |\eta_{Spe} + \Delta\eta|}$$

  - **CALO energy uncertainty ±ε is symmetric for e^- and e^+;**
  - **spectrometer global distortion Δη gives a charge-sign dependent effect.**
  - **evaluated $\Delta\eta \sim -10^{-3}\ GV^{-1}$**

Measurement of |Z|

$$-\frac{dE}{dx} = Kz^2\frac{Z}{A}\frac{1}{\beta^2}\left[\frac{1}{2}\ln\frac{2m_ec^2\beta^2\gamma^2T_{\max}}{I^2} - \beta^2 - \frac{\delta(\beta\gamma)}{2}\right]$$

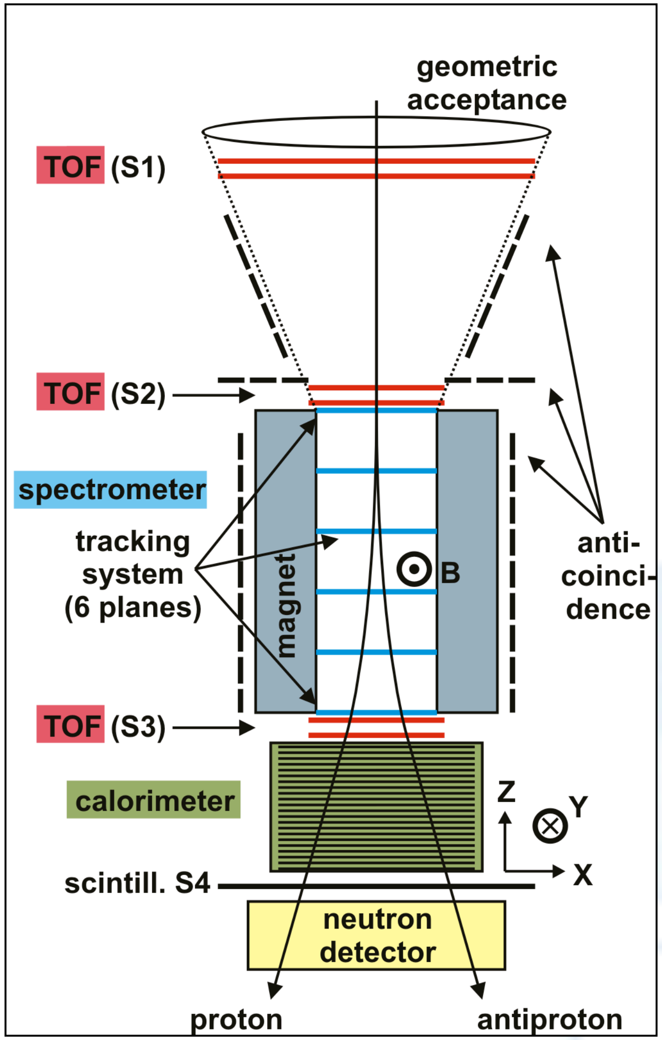

Bethe-Bloch
ionization energy-loss of heavy ($M>>m_e$) charged particles (TOF, TRK, CALO)

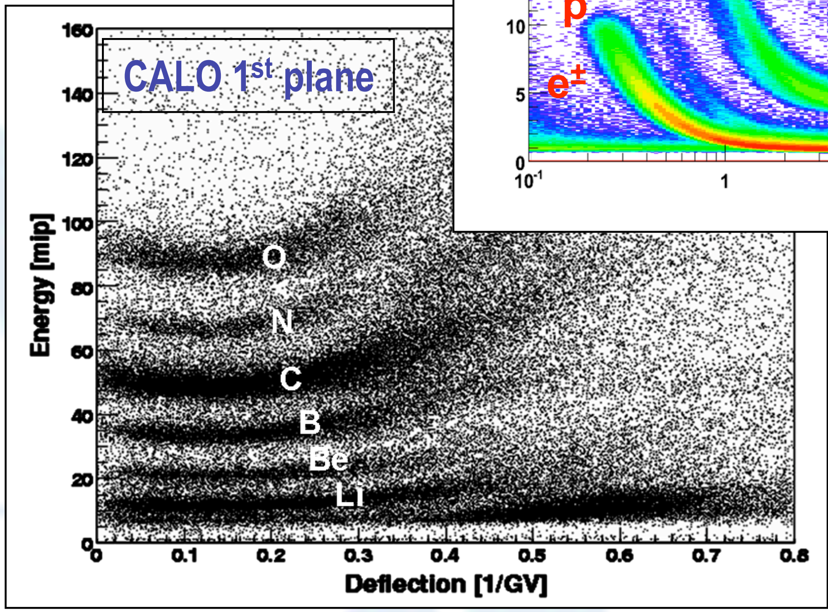

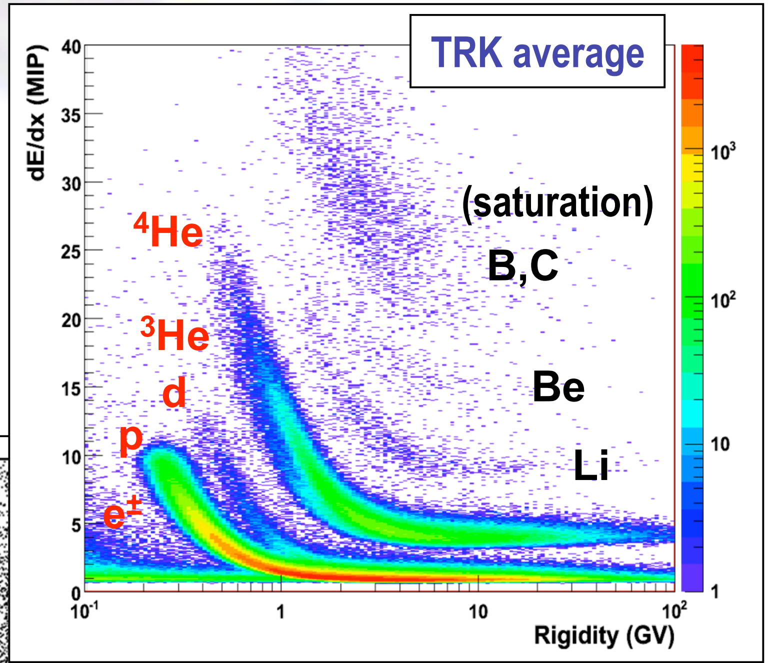

Measurement of velocity β

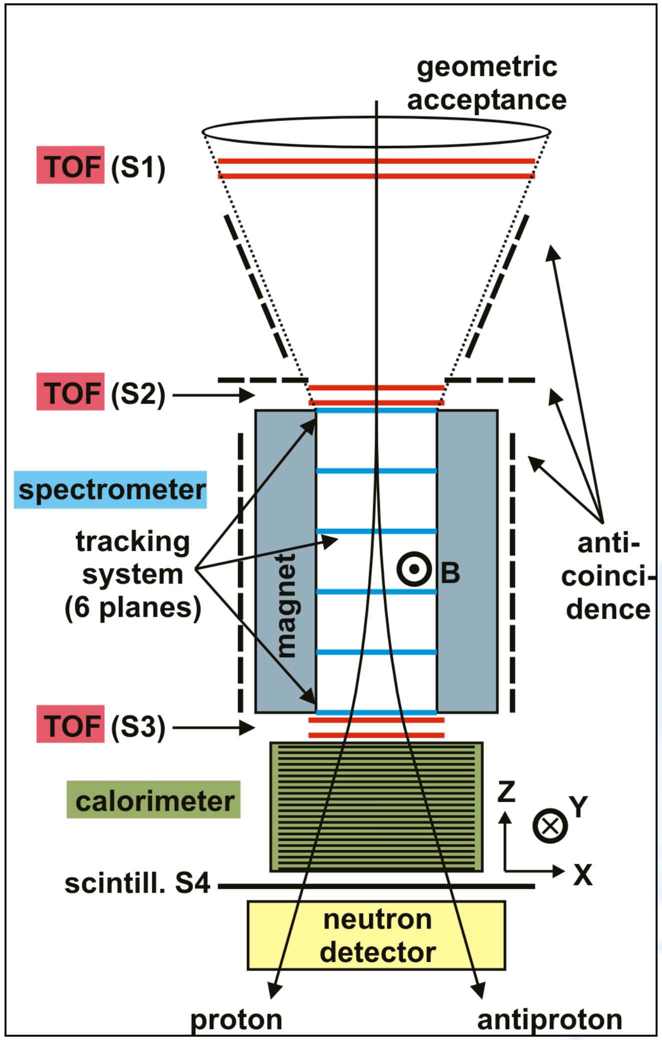

TOF (Time-of-Flight)

- 3 double plastic scintillator planes.

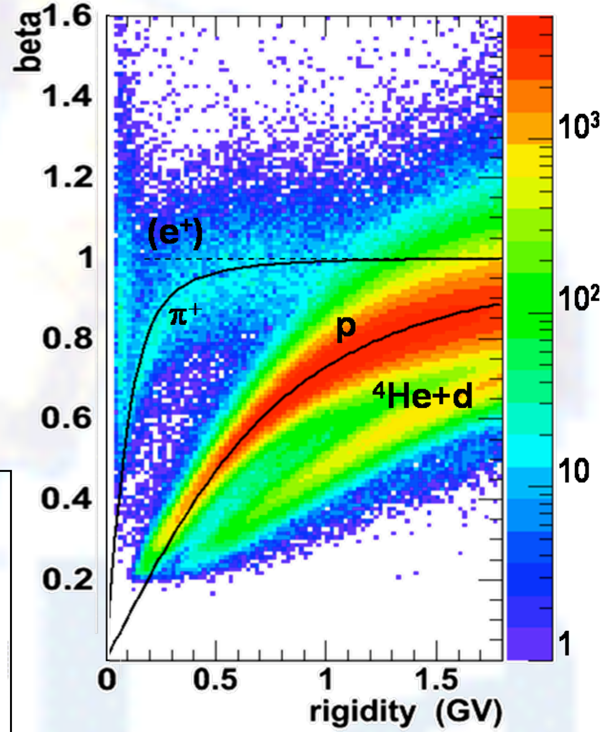

- Particle identification at low energy.
- Several independent β measurements.

- Reject upward going particles, which mimic downward-going antiparticles.
- 300 ps TOF resolution vs. 3 ns flight time.

- Give trigger to the apparatus.
- With double layers, trigger efficiency (~100%) is measured with in-flight acquired data.

Discrimination between e^+/e^- and hadron

Electromagnetic sampling CALO

hadron (R=19GV)

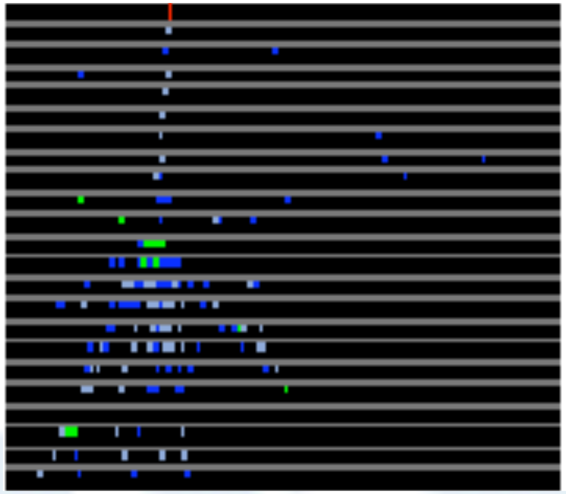

- 22 modules: Y Si-strip + W layer + X Si-strip.

- Total depth: 16.3 X_0 or 0.6 λ_I.

- Longitudinal and lateral segmentation.
- dE/dL from single strips.
- Clear imaging of interaction topology.

electron (R=17GV)

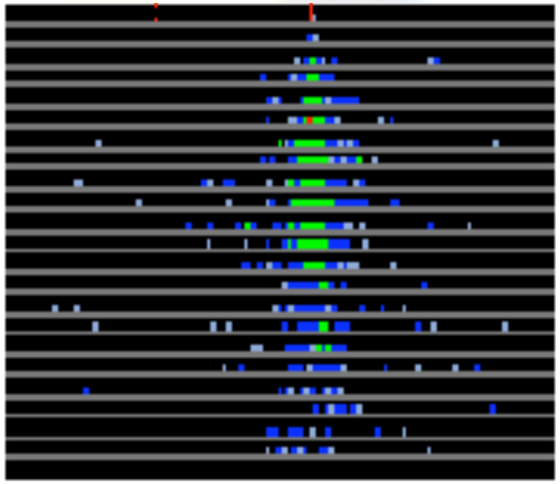

Energy measurement of electrons and positrons (~full shower containment)

$$\frac{\sigma_E}{E} = a \oplus \frac{b}{\sqrt{E}} \qquad a < 5\%$$

Amount of neutrons in ND helps discrimination

PAMELA nominal capabilities

Particle	Energy range (with 3 years statistics)
• Antiprotons	80 MeV - 190 GeV
• Protons	up to 700 GeV
• Positrons	50 MeV - 270 GeV
• Electrons	up to 400 GeV
• Electrons+positrons	up to 2 TeV (without charge sign)
• Light Nuclei	up to 200 GeV/n (He/Be/C)
• Antinuclei search	

Upper limits from TRK rigidity measurement (antiprotons, protons)

Upper limits from CALO lepton/proton discrimination (positrons, electrons)

Simultaneous measurement of many cosmic-ray species.

New energy range.

Unprecedented statistics.

Typical PAMELA events

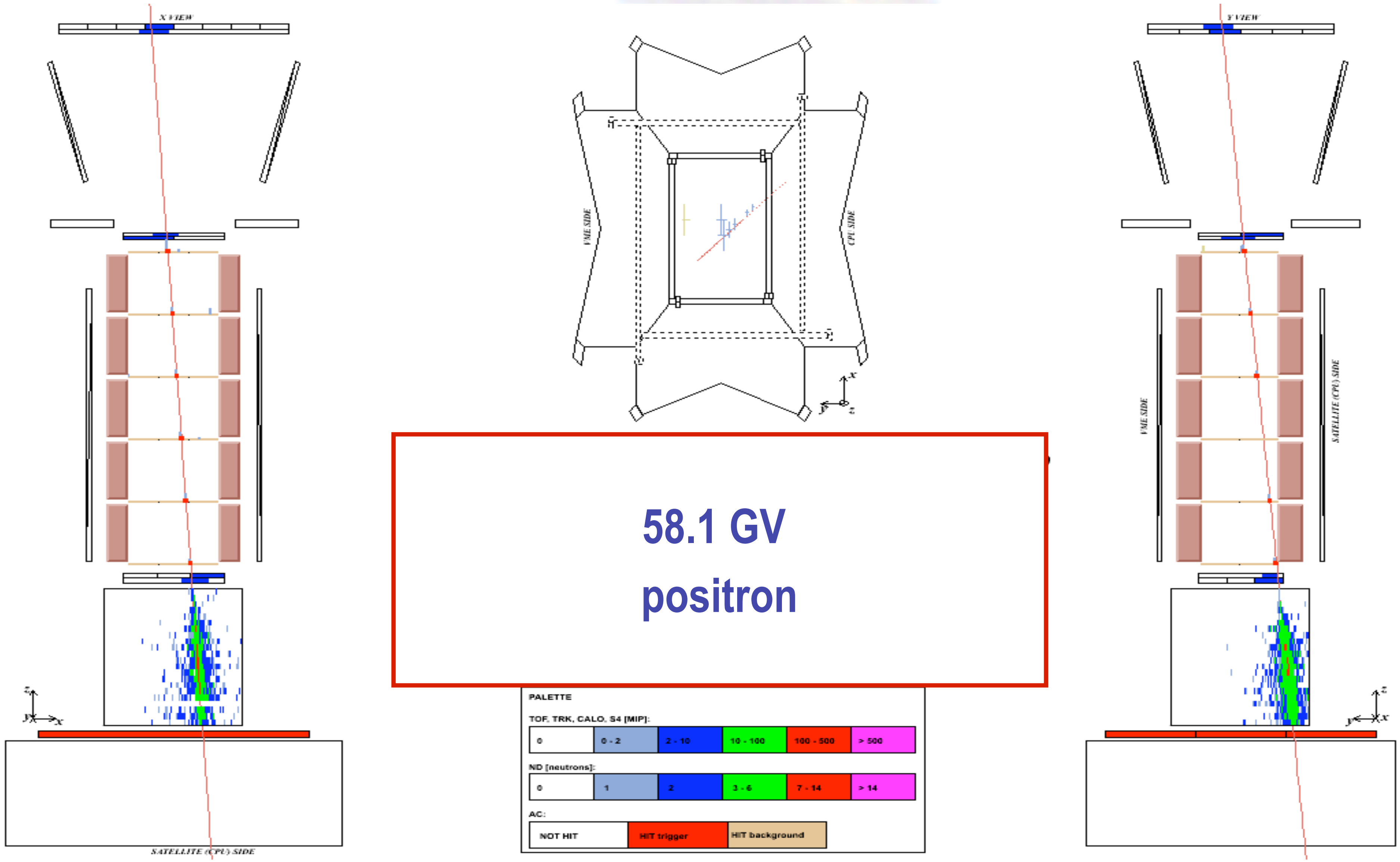

58.1 GV

positron

36 GV interacting proton

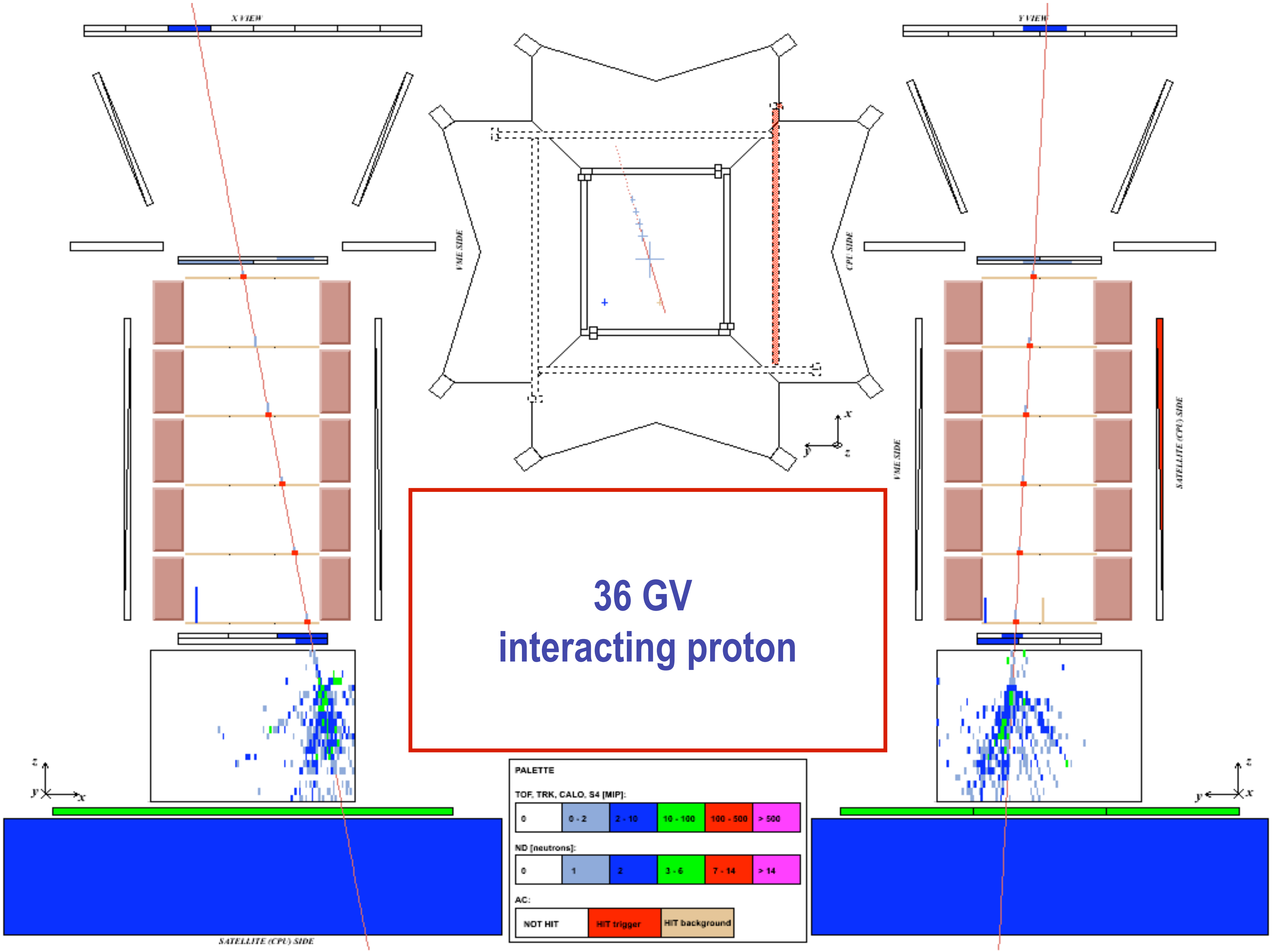

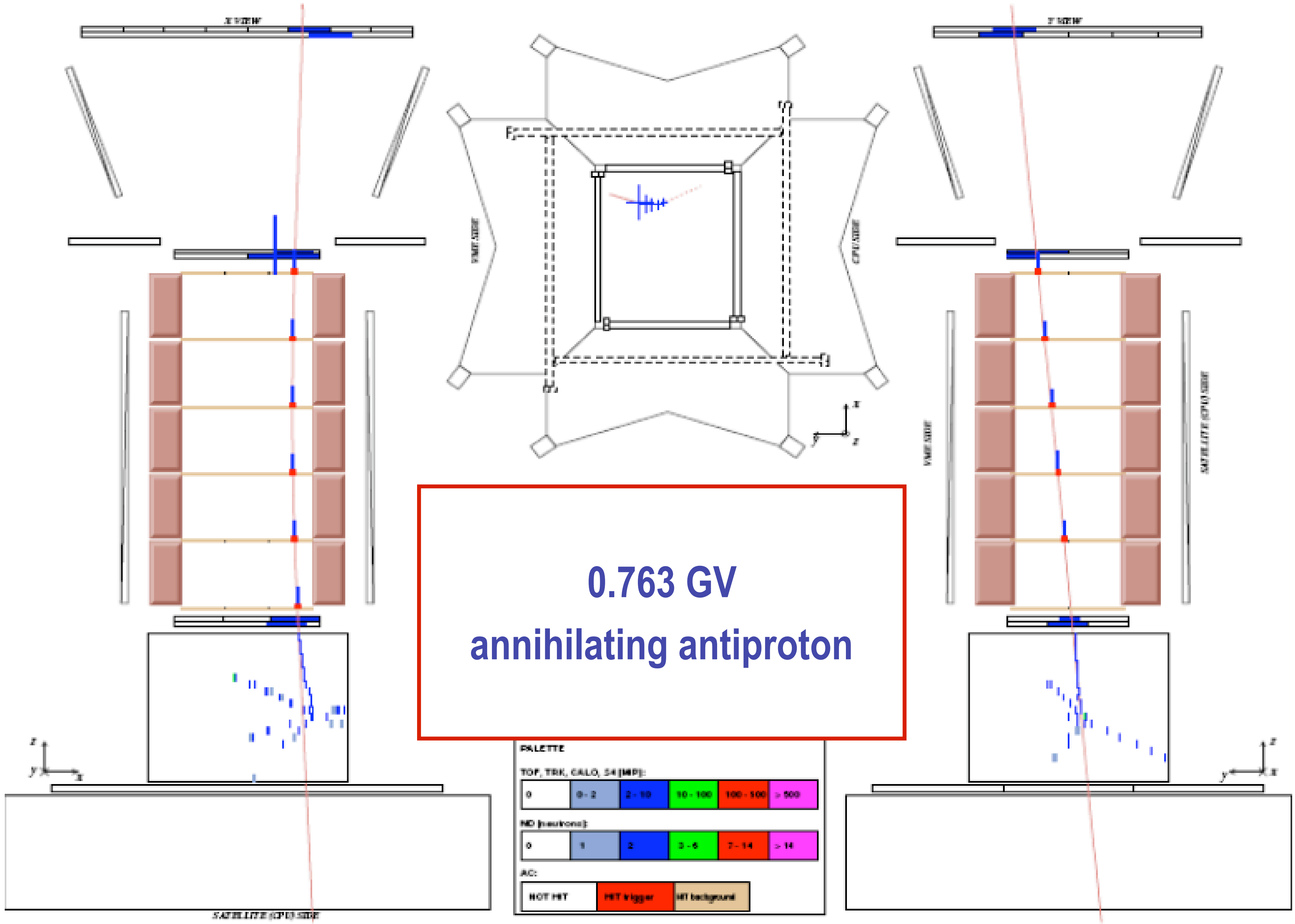

0.763 GV

annihilating antiproton

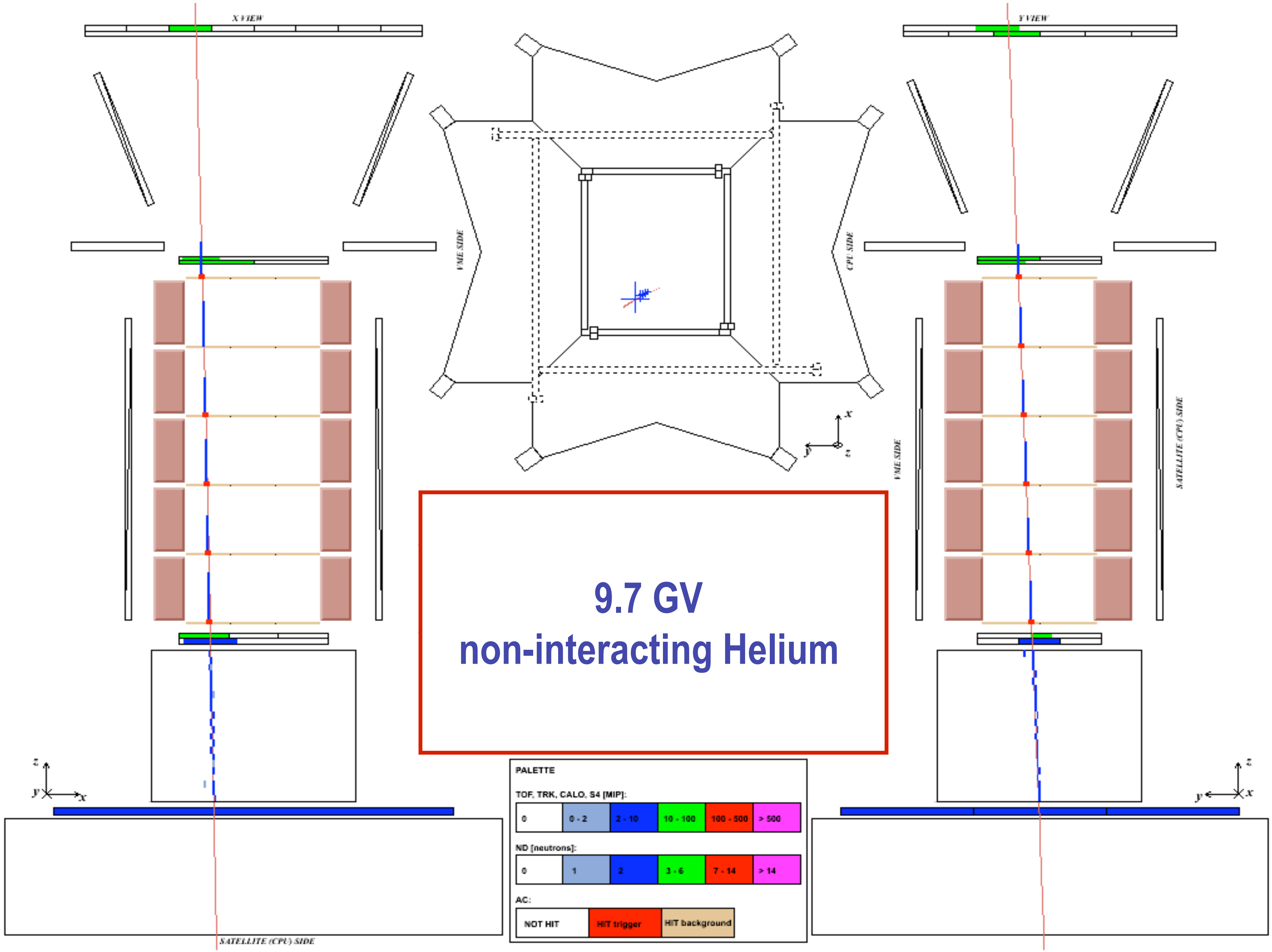
X VIEW
Y VIEW
VME SIDE
CPU SIDE
SATELLITE (CPU) SIDE
9.7 GV
non-interacting Helium
PALETTE
TOF, TRK, CALO, S4 [MIP]:
0
0 - 2
2 - 10
10 - 100
100 - 500
> 500
ND [neutrons]:
0
1
2
3 - 6
7 - 14
> 14
AC:
NOT HIT
HIT trigger
HIT background

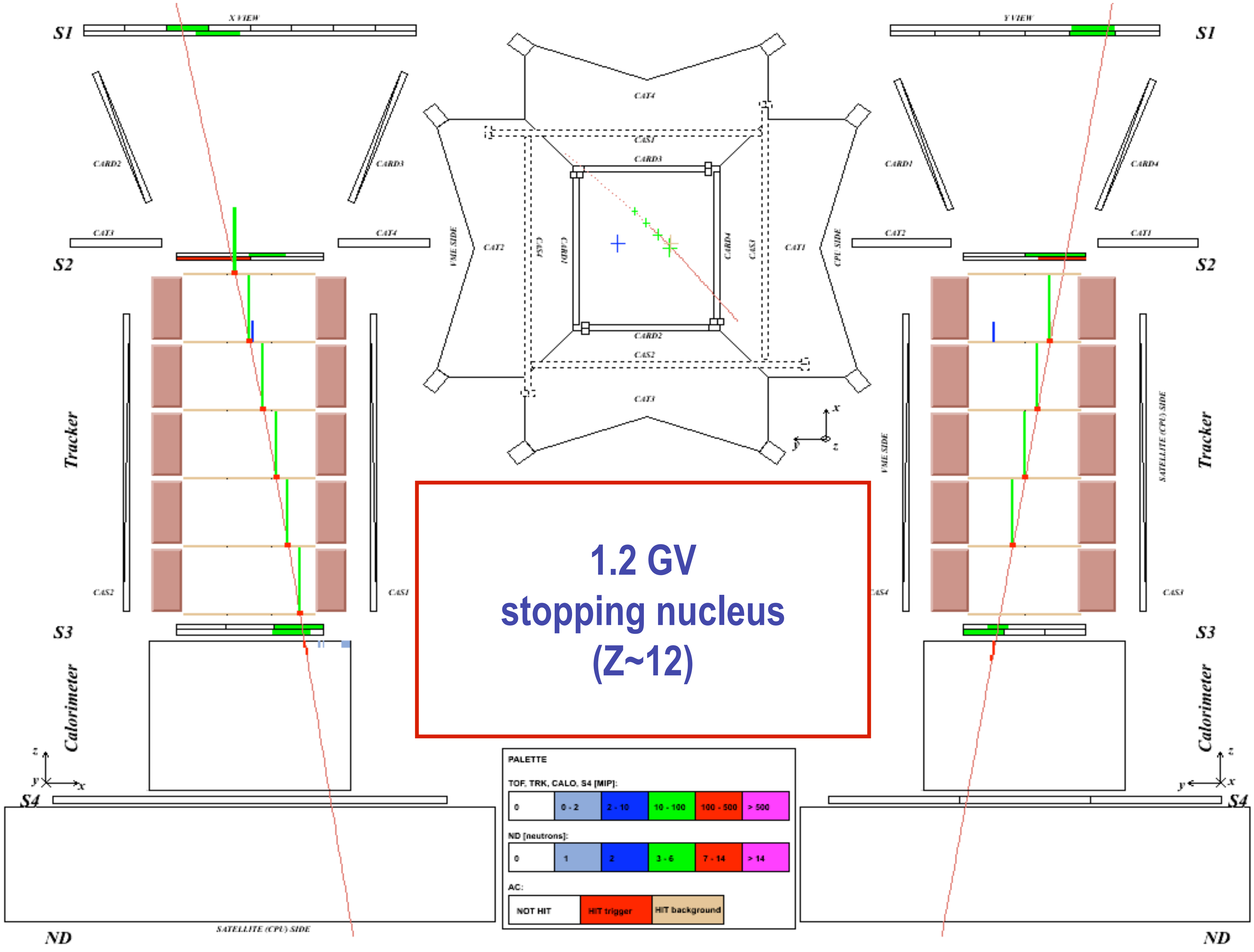

1.2 GV
stopping nucleus
(Z~12)
S1
S2
S3
S4
ND
Tracker
Calorimeter
X VIEW
Y VIEW
CARD1
CARD2
CARD3
CARD4
CAT1
CAT2
CAT3
CAT4
CAS1
CAS2
CAS3
CAS4
VME SIDE
CPU SIDE
SATELLITE (CPU) SIDE
PALETTE
TOF, TRK, CALO, S4 [MIP]:
0
0 - 2
2 - 10
10 - 100
100 - 500
> 500
ND [neutrons]:
0
1
2
3 - 6
7 - 14
> 14
AC:
NOT HIT
HIT trigger
HIT background

(2) Measurement of relative fluxes of antiparticles

Relative vs. absolute antiparticle fluxes

- **The absolute differential flux of a particle species in a given energy bin is defined:**

$$J(bin) = \frac{N_{SEL}}{T_{LIVE}} \cdot \frac{1}{\varepsilon_{TRIG}} \cdot \frac{1}{\varepsilon_{SEL}} \cdot \frac{1}{E_{\max} - E_{\min}} \cdot \frac{1}{G}$$

and measured in particles/(s ≅ GeV ≅ m^2 sr), with:

  - **N_{SEL} : number of selected events, during the live time T_{LIVE} (s), giving trigger and satisfying a set of selection cuts which ideally reject all unwanted background.**
  - **ε_{TRIG} : trigger efficiency.**
  - **ε_{SEL} : combined efficiency of all the selection cuts.**
  - **G: geometric factor (m^2 sr) for the instrument acceptance.**

- **Dependence of all quantities from the bin (energy) is implicit.**

- **All the involved factors and their energy dependence must be measured.**

Relative vs. absolute antiparticle fluxes

- **Relative differential fluxes of antiparticles:**
  - (2.a) proton/antiproton flux ratio;
  - (2.b) positron fraction over the positron+electron flux.

  exploit the fact that particle and antiparticle behave almost identically in the detectors.

- **If the same selection cuts are used** for antiparticle and particle, then the relative fluxes are given by ratios of selected events:

$$R(bin) = \frac{N_{SEL}^{(p-bar)}}{N_{SEL}^{(p)}}$$

$$F(bin) = \frac{N_{SEL}^{(e^+)}}{N_{SEL}^{(e^+ + e^-)}}$$

  - systematic errors related to all other terms are thus avoided;
  - residual differences in interactions are taken into account as (small) corrections.

(2.a) Antiproton/proton ratio

Antiproton/proton analysis

- **This analysis is used here as a first illustrative template of the general approach to measure particle fluxes with PAMELA.**

- **Three main steps:**
  - **(Step I) basic event selection;**
  - **(Step II) p-bar/e^- discrimination with CALO;**
  - **(Step III) p-bar/p separation with TRK (the main issue).**

(Step I) Basic event selection

- **Aim of the selection cuts:**
  - **reject background;**
  - **guarantee a precise measurement of rigidity R.**
- **All cuts are applied for both charge signs.**

- **Clean event pattern:**
  - **single track satisfying minimal TRK requirements (discussed later);**
  - **no activity in CARD+CAT.**
- **$|Z|=1$ from dE/dL vs. R.**

- **β vs. R consistent with m_p (at energies < m_p):**
  - **reject pions from interaction.**

- **Downward-going particle (TOF β).**
- **$R > 1.3\ R_{cutoff}$ (Stoermer vertical geomagnetic cutoff):**
  - **conservatively reject reentrant (non-galactic) particles.**

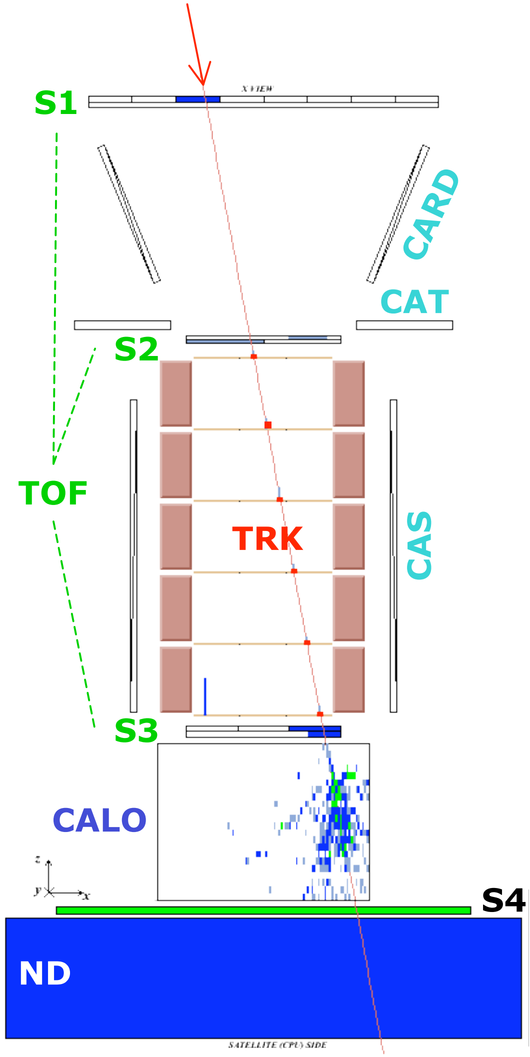

Geomagnetic cutoff

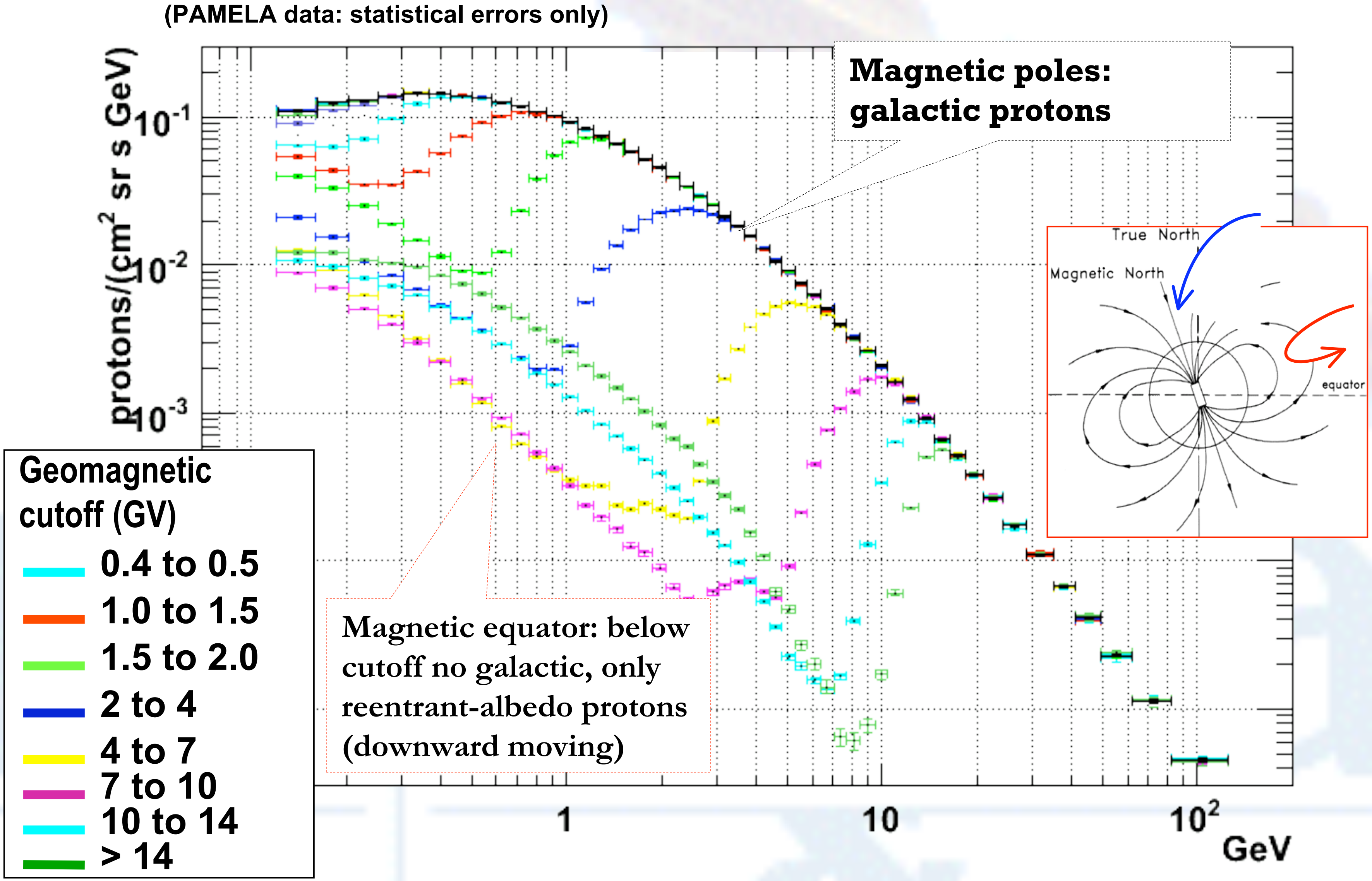

S. Ricciarini ***EPA 09***

Momentum and charge sign with TRK

- **Minimal track requirements for good rigidity measurement:**
  - at least 4 X (bending view) + 3 Y hits;
  - energy-dependent cut on track χ^2 (~95% total efficiency);
  - consistent TRK+TOF+CALO spatial information.

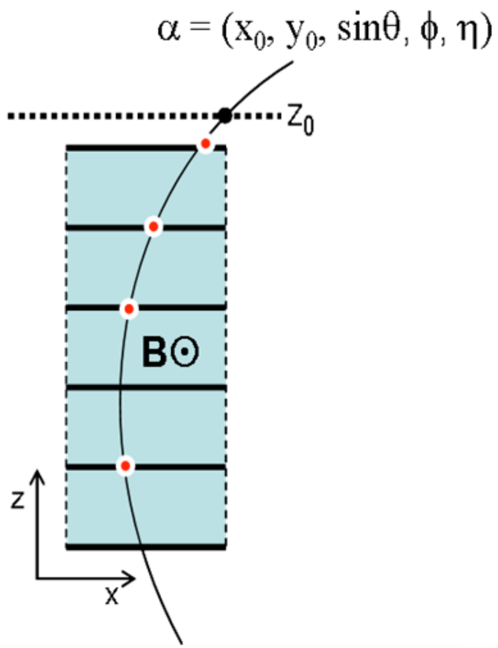

Magnetic rigidity R = pc/Ze (GV)
Magnetic deflection $\eta = 1/R$ (GV^{-1})

MDR (Maximum Detectable Rigidity)
MDR=$1/\sigma_\eta$ (σ_η spectrometer deflection resolution)

MDR depends on event characteristics and is evaluated event-by-event with the fitting routine:

- number and distribution of fitted points along the track;

- spatial resolution of the single position measurements (varies with track inclination and strip noise);

- magnetic field intensity along the track.

(Step II) p-bar/e$^-$ discrimination

- **Contamination from e$^-$ on p-bar sample is reduced to a negligible amount.**
  - **e$^-$ are easily identified in CALO from interaction topology:**
    - **interact in the first CALO layers;**
    - **give well contained, compact EM showers;**
  - **on the other hand, most hadrons interact well deep in the CALO or do not interact at all.**

hadron (R=19GV)

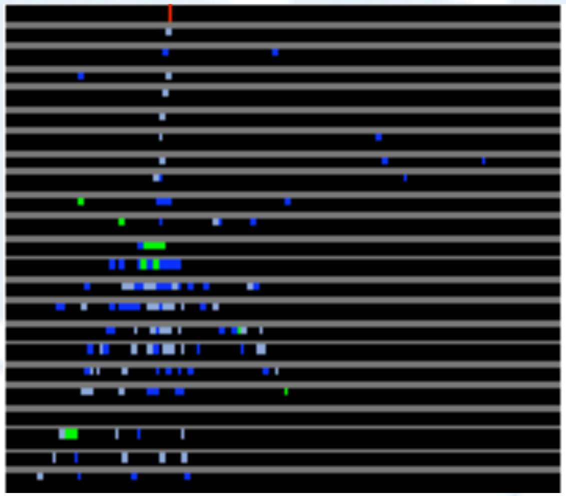

electron (R=17GV)

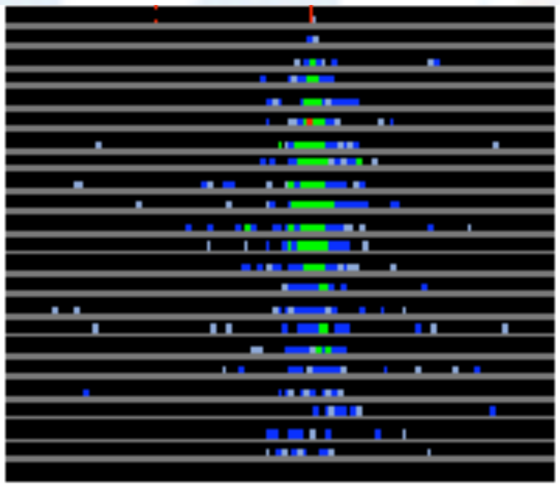

22 modules (Y Si-strip + W layer + X Si-strip)

Total depth:
16.3 X_0 or 0.6 λ_I

p-bar/e⁻ discrimination

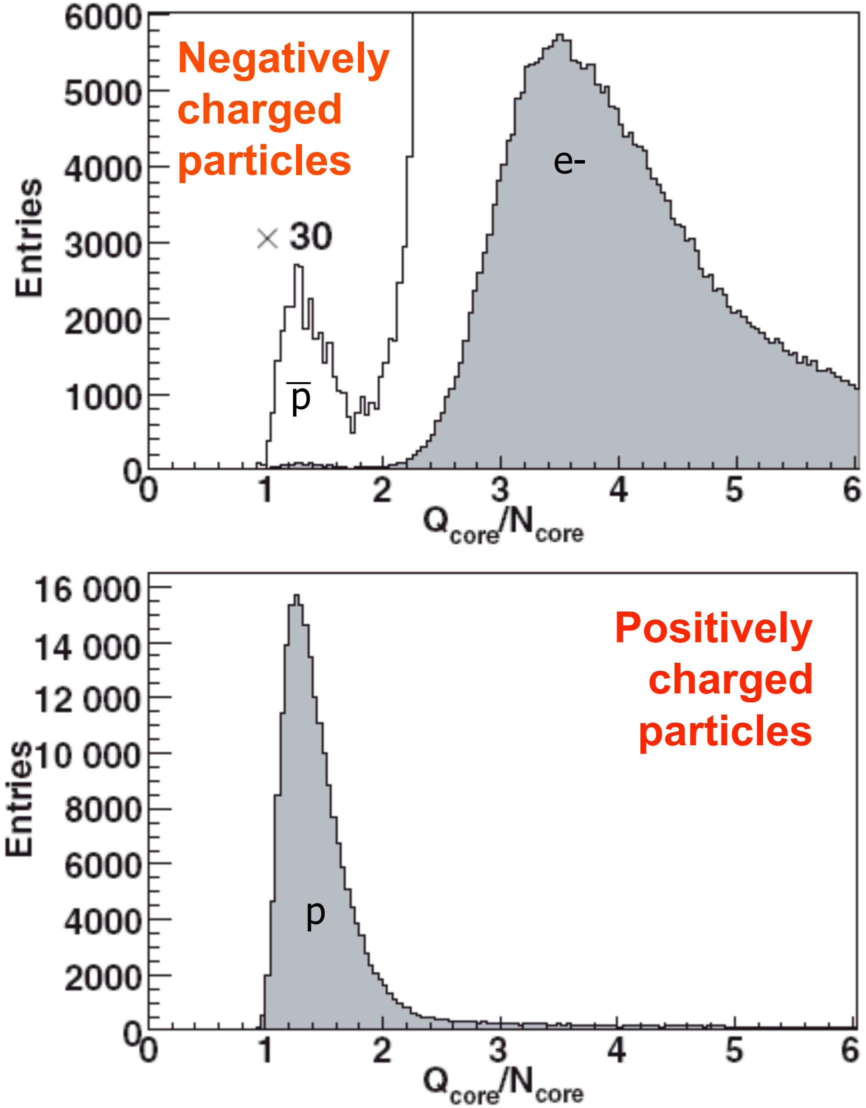

- The CALO offers an excellent discrimination between electromagnetic and hadronic interactions.
- Several topological variables can be defined.
- As example, the energy density in the shower core weighted by the depth in the calorimeter.
- Total rejection factor $>10^4$ for e^- from beam tests and simulation.
- Residual e^- contamination after all topological cuts are applied is negligible.

Selected sample after all previous cuts

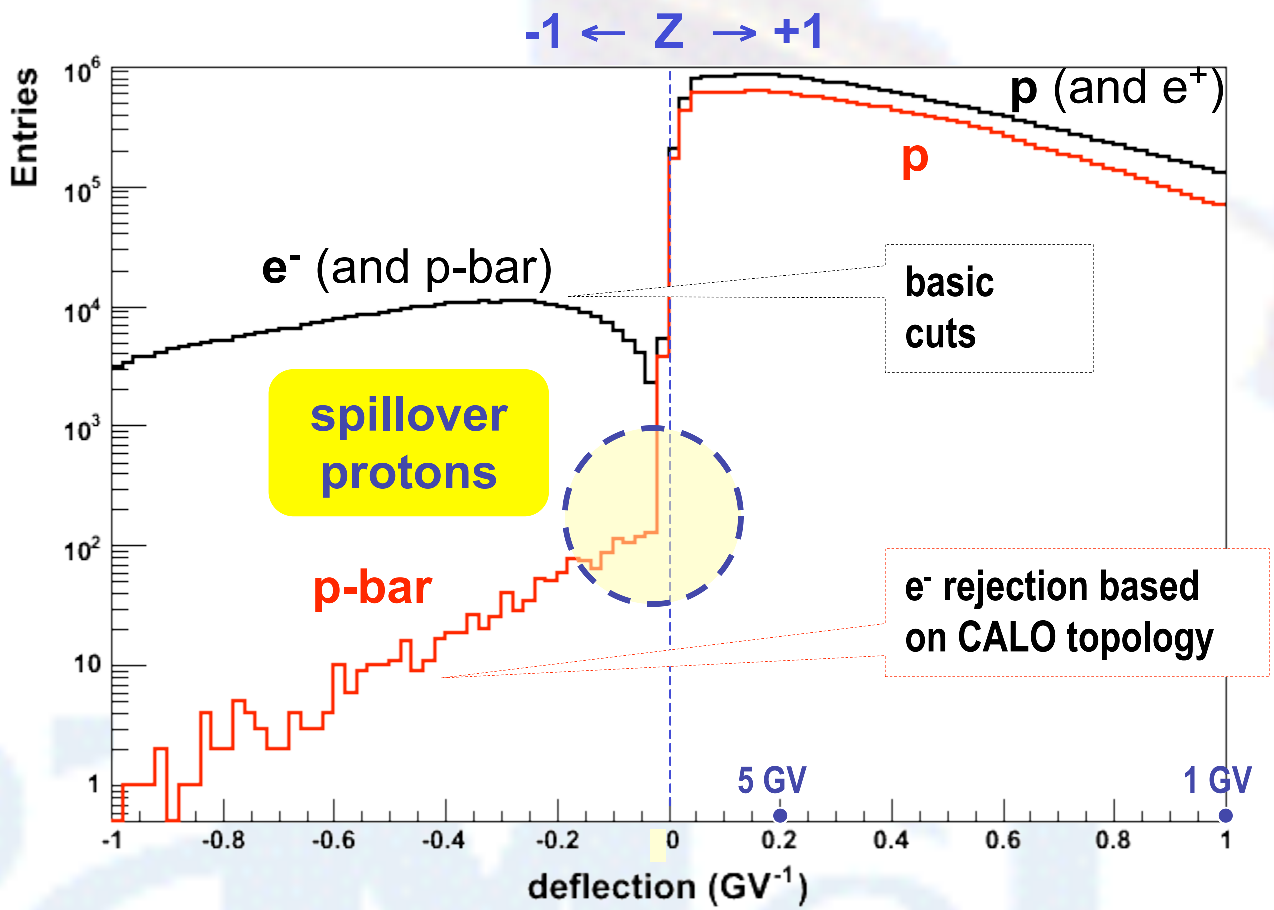

- **At high energies the p-bar sample can contain "spillover" protons (i.e. with wrong measured charge sign), as consequence of the deflection uncertainty σ_η=1/MDR.**

(Step III) p-bar/p charge-sign separation

- Spillover proton background is the main issue for this analysis, because of the high (~ 10^4) p/p-bar ratio in cosmic rays.
  - Defined a set of additional optimized TRK requirements to improve MDR of selected events.

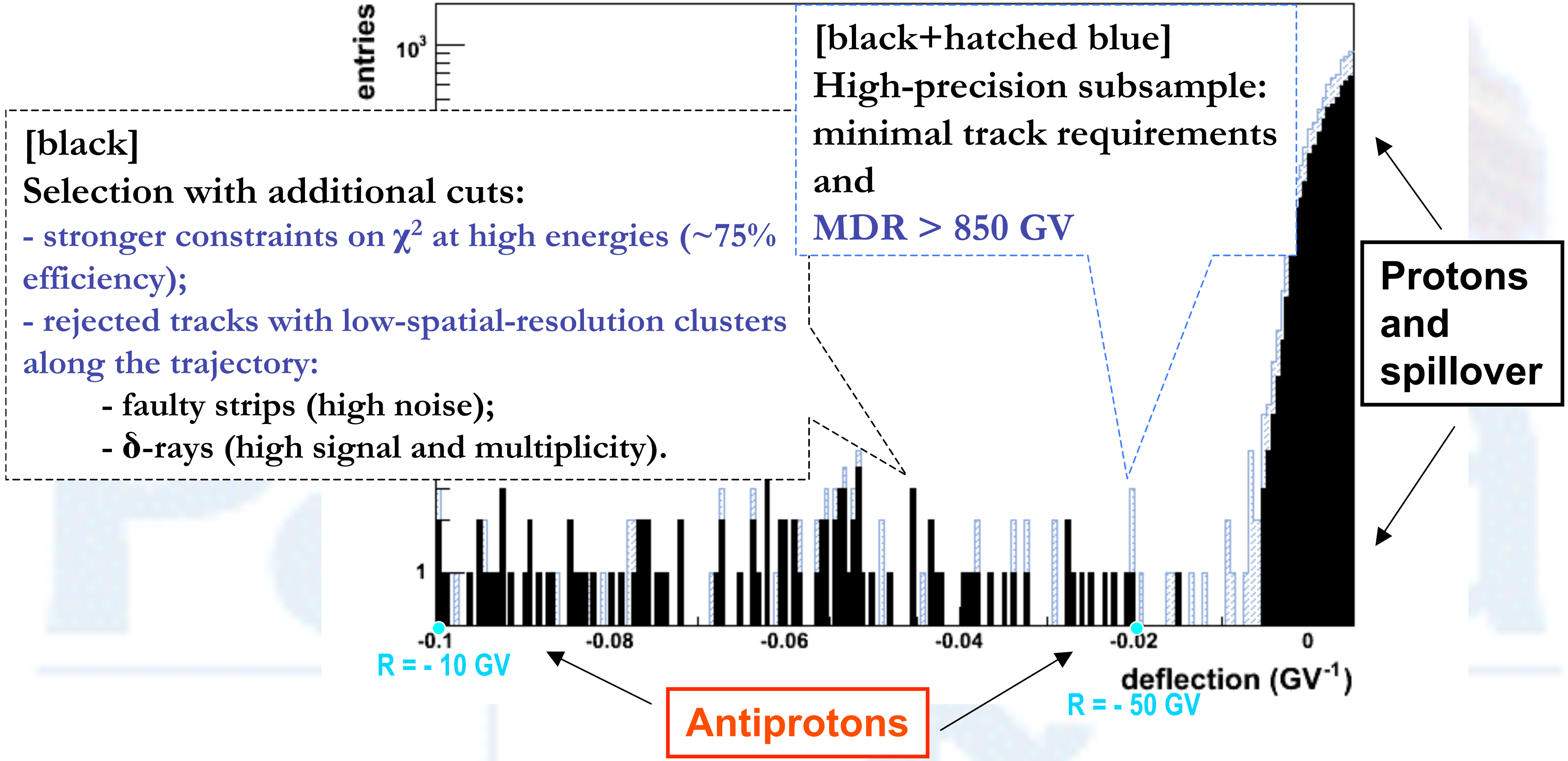

p-bar/p charge-sign separation

Further additional rigidity-dependent cut to reject residual spillover:
MDR > 10 · |R| or equivalently |η| > 10 · σ_η

Residual spillover contamination is finally reduced to a negligible amount.

subsample with MDR > 850 GV (used for cut study and optimization) ↑

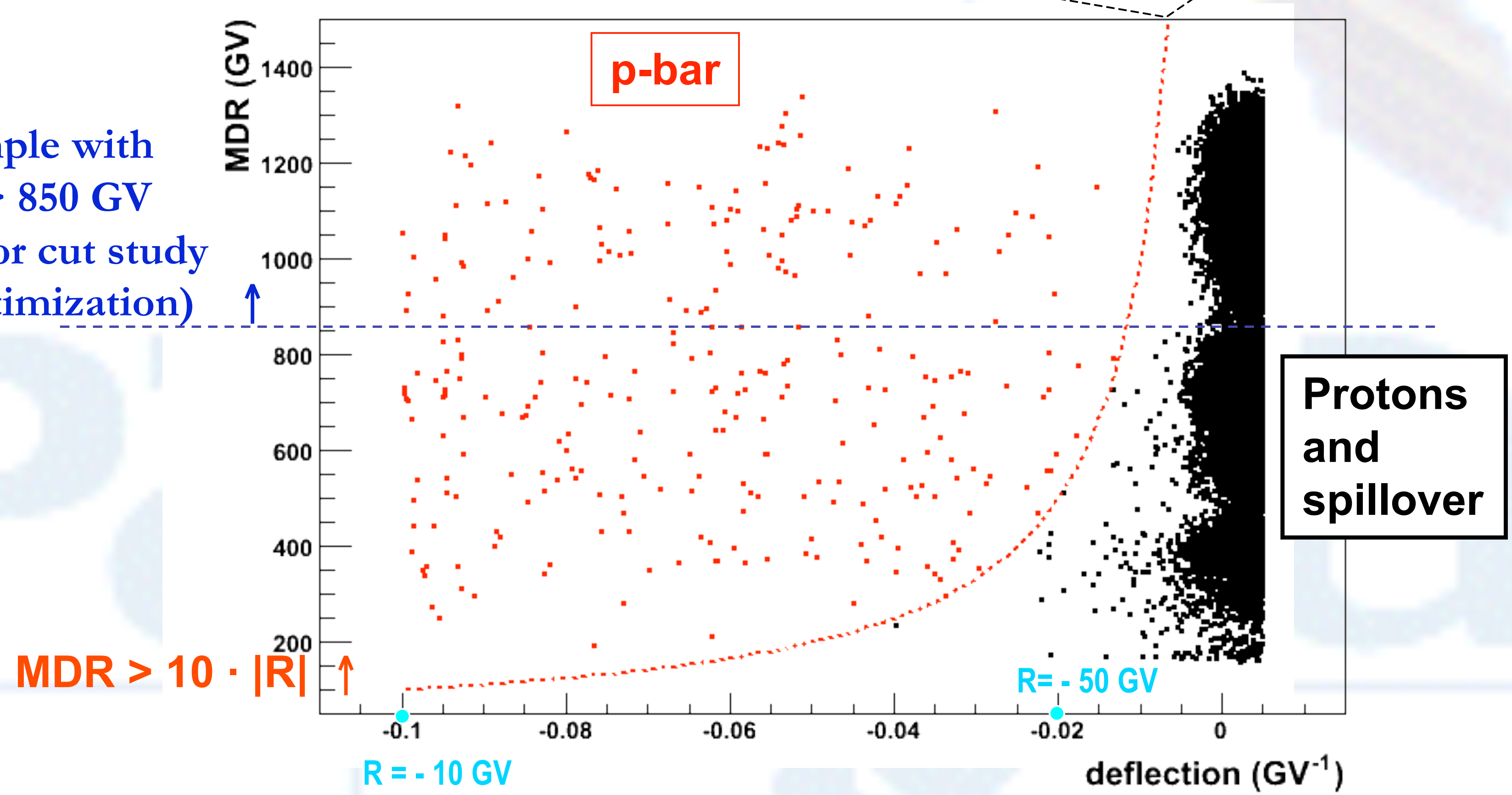

Antiproton/proton ratio (PRL 102, 2009)

- **Excellent agreement with recent data from other experiments.**
  - One order of magnitude improvement in statistics.
  - Most extended energy range ever achieved.
- **Correction factors are included and ~ one order of magnitude less than statistical error.**
  - CALO efficiency (different for p-bar and p);
  - loss of particles for interactions.
- **Not included but negligible: residual π contamination**

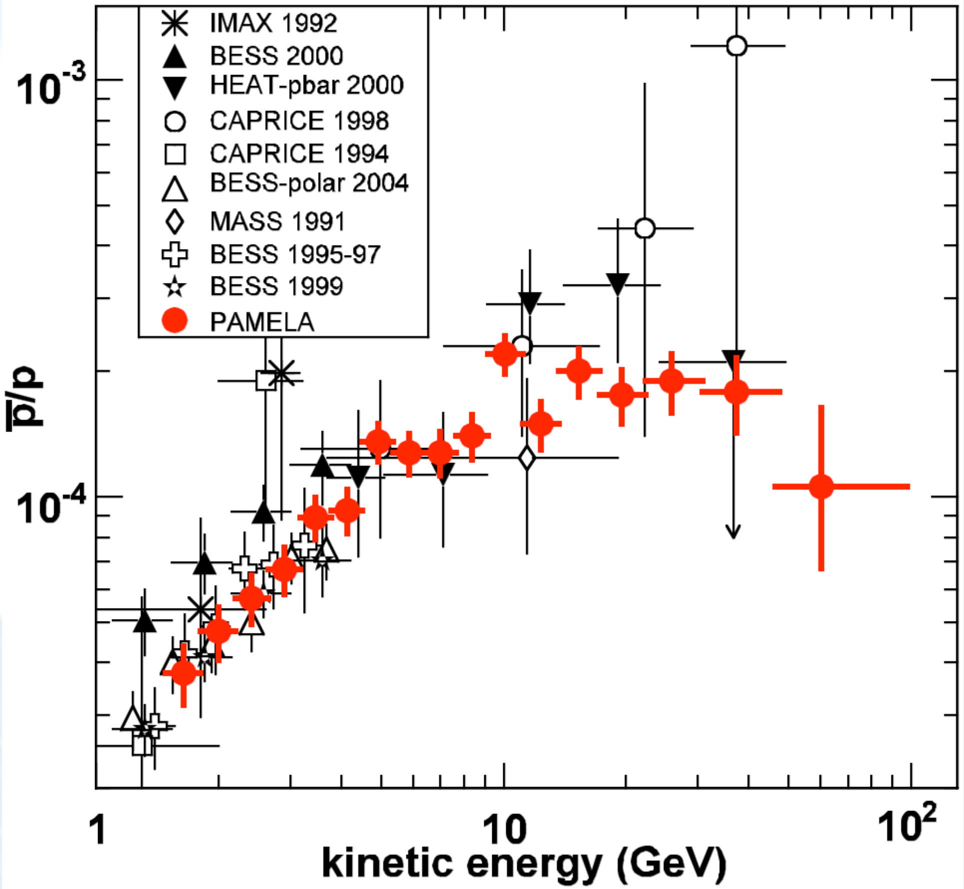

Antiproton/proton ratio (PRL 102, 2009)

- **Ratio increases smoothly with energy from 4 x 10^{-5} and levels off at ~ 1 x 10^{-4}.**
- **Our results are enough precise to place tight constraints on parameters relevant for secondary production calculations.**
- **Our data above 10 GeV place limits on contributions from exotic sources, e.g. dark matter particle annihilations.**

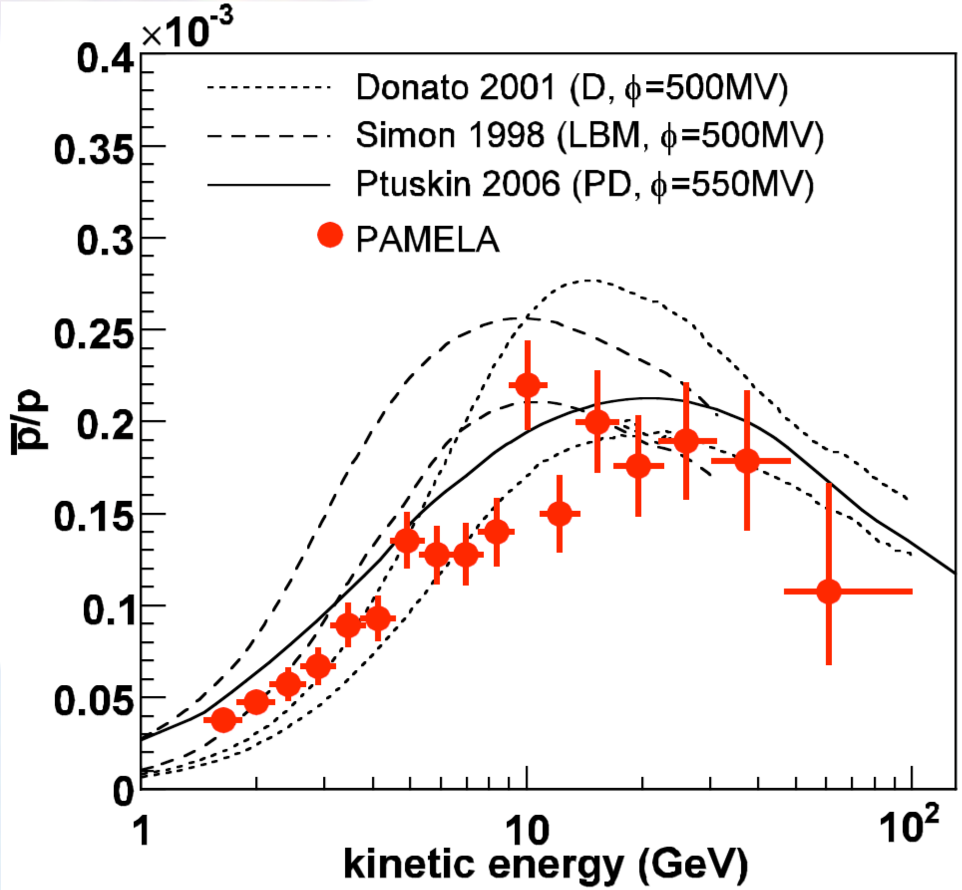

New preliminary antiproton/proton ratio

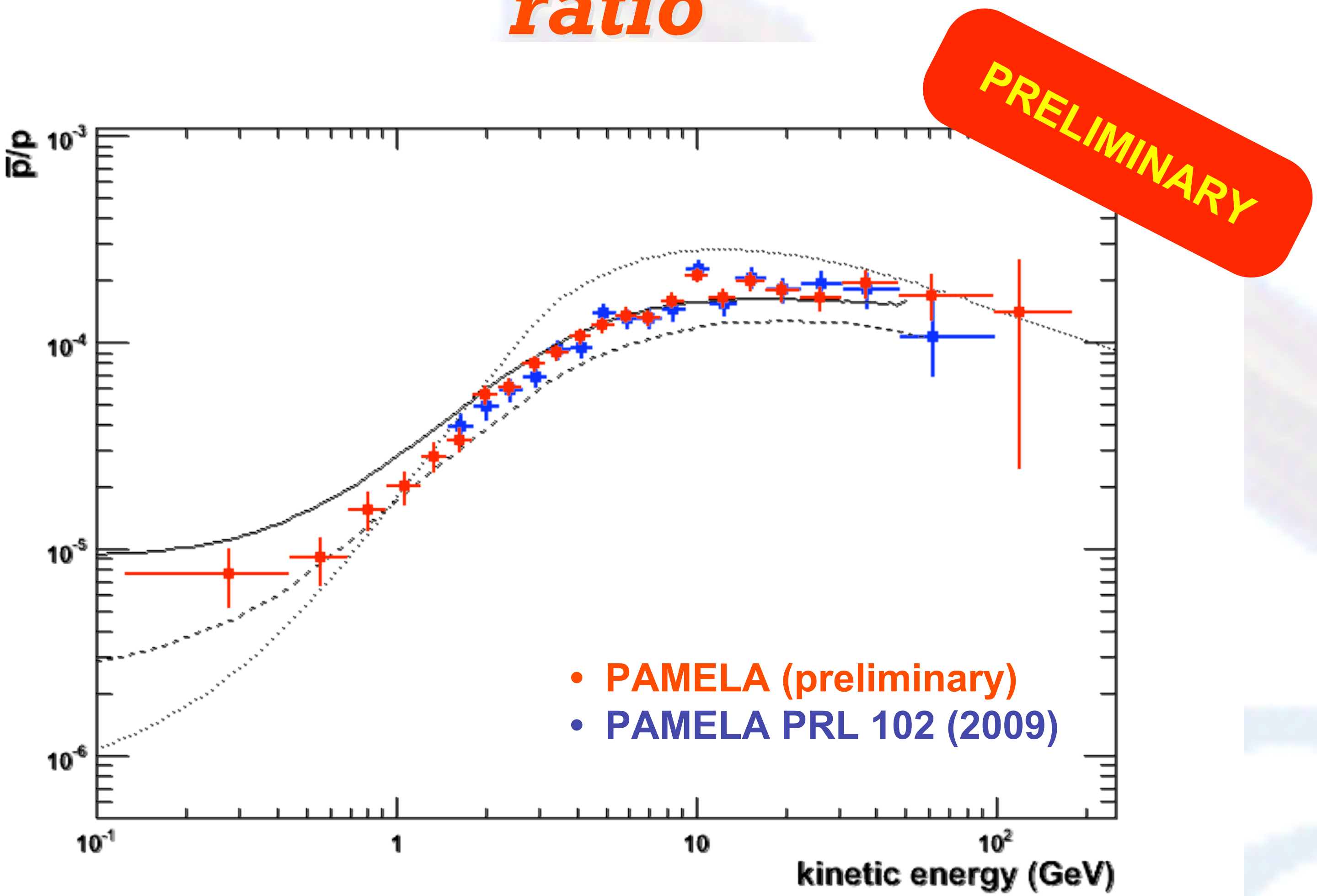

- **Included further collected statistics.**
- **Energy range extended in both directions.**
- **New analysis points are fully consistent with old ones.**

New preliminary antiproton/proton ratio

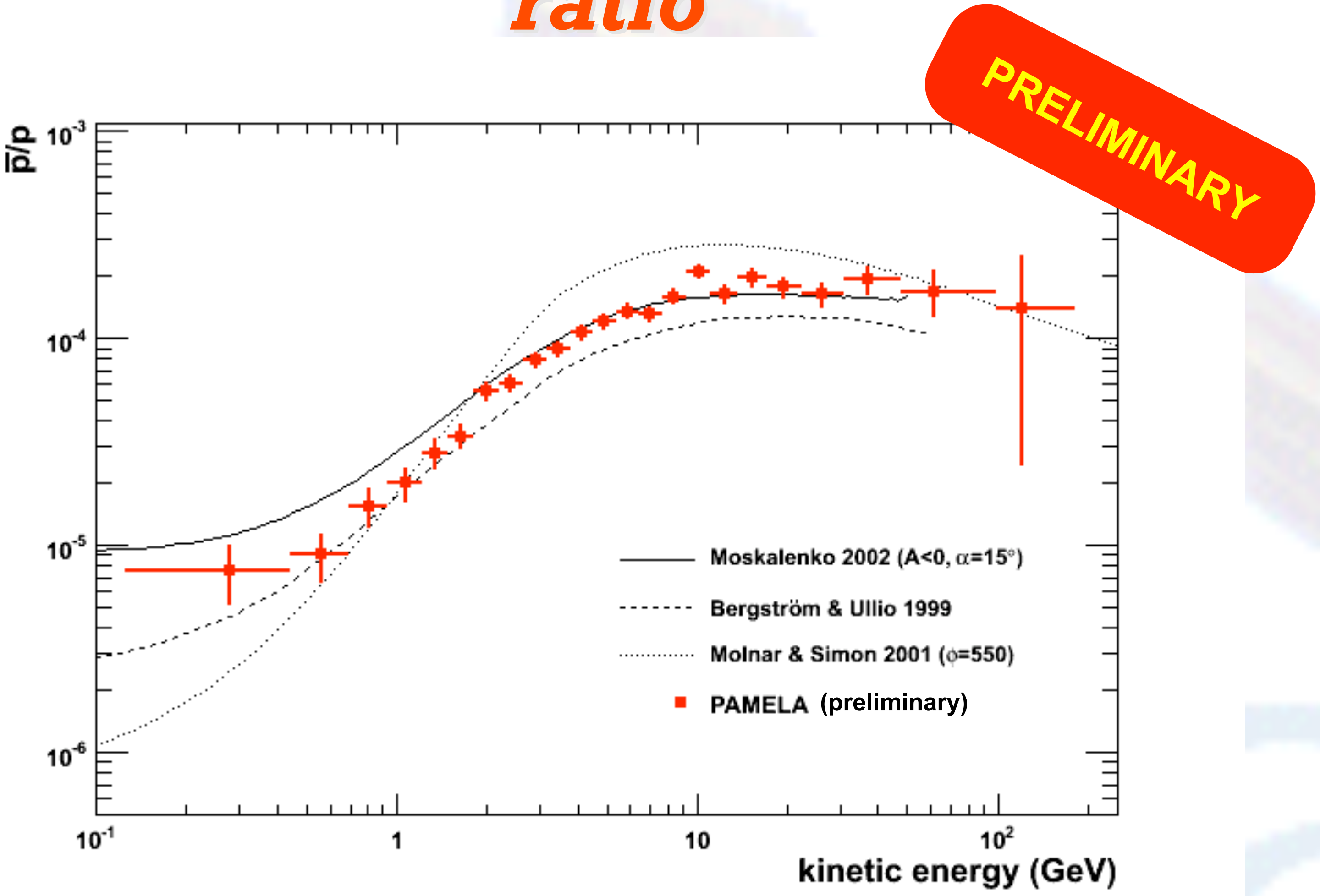

- **For the highest bin, the cut MDR > 6 · |R| is used to increase statistics.**
  - **Estimation of spillover background is under way.**

(2.b) Positron fraction

High-energy positron fraction analysis

- **Results discussed here have been published in *Nature 458 (2009), 607-609*.**

- **Analyzed data: July 2006 - February 2008.**
- **Total acquisition time ~ 500 days.**
- **~ $1 \cdot 10^9$ triggers (~ 8.8TB of data).**

- **Identified ~150×10^3 electrons and ~9×10^3 positrons with energy between 1.5 and 100 GeV.**
  - **Collected 180 positrons above 20 GeV.**

- **Analysis of new data with extension of energy range in both directions is under way.**

High-energy positron fraction analysis

- Basic cuts: similar to antiproton/proton ratio.
- Rigidity measured by TRK.
  - Brehmsstrahlung inside spectrometer taken into account (cross-check with CALO energy measurement).
- e^-/e^+ charge-sign separation (spillover rejection) is much easier than for p-bar/p:
  - e^-/e^+ ratio is relatively small at high energies (~10) with respect to p/p-bar (~10^4).
- Main issue for this analysis: e^+/p separation with CALO.
  - $\pi^0 \rightarrow \gamma\gamma$ from hadronic showers might mimic pure EM showers;
  - p/e^+ ratio increases for increasing energy (10^3 at 1 GV; 10^4 at 100 GV).

e^+/p separation with CALO

- **Positron identification based on:**
  - **total detected energy** (**"energy-rigidity match"**);
  - **shower topology** (**lateral and longitudinal profile, shower starting point**).

51 GV positron

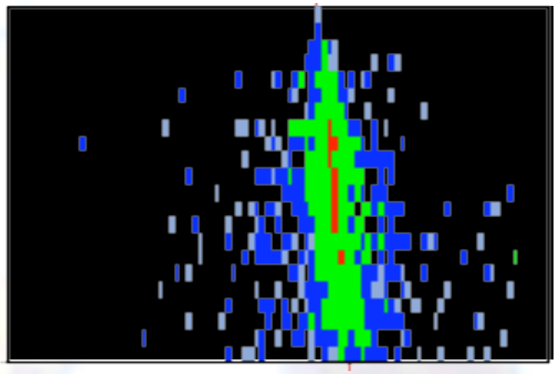

- **Procedure can be divided into 2 steps.**

80 GV proton

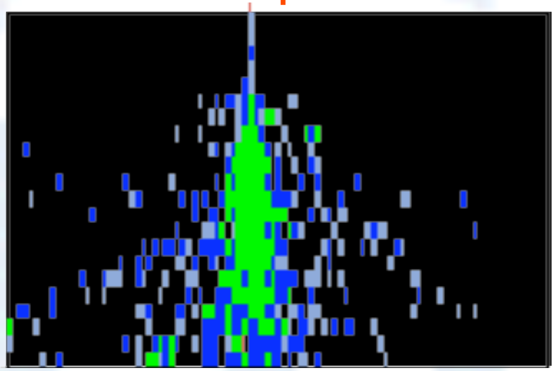

- ***(Step I) p background suppression with CALO.***
  - **The required p rejection factor is larger than 10^5.**
- ***(Step II) evaluation of residual p background.***
  - **Given the importance of the measurement, this evaluation is based only on flight data.**
  - **Beam-test and/or simulation calibrations are not introduced in the measurement, but used for cross-check purposes.**

(Step 1) Background suppression with CALO

Fraction *F* of energy released in CALO along the track in a cylinder of radius $0.3\ r_{Molière}$ (central + 2 lateral Si strips)

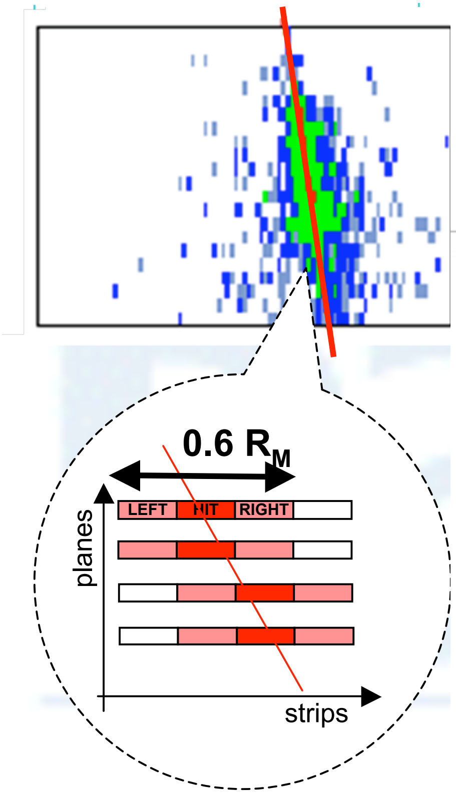

Rigidity: 20-30 GV

after basic event cuts,
before CALO cuts

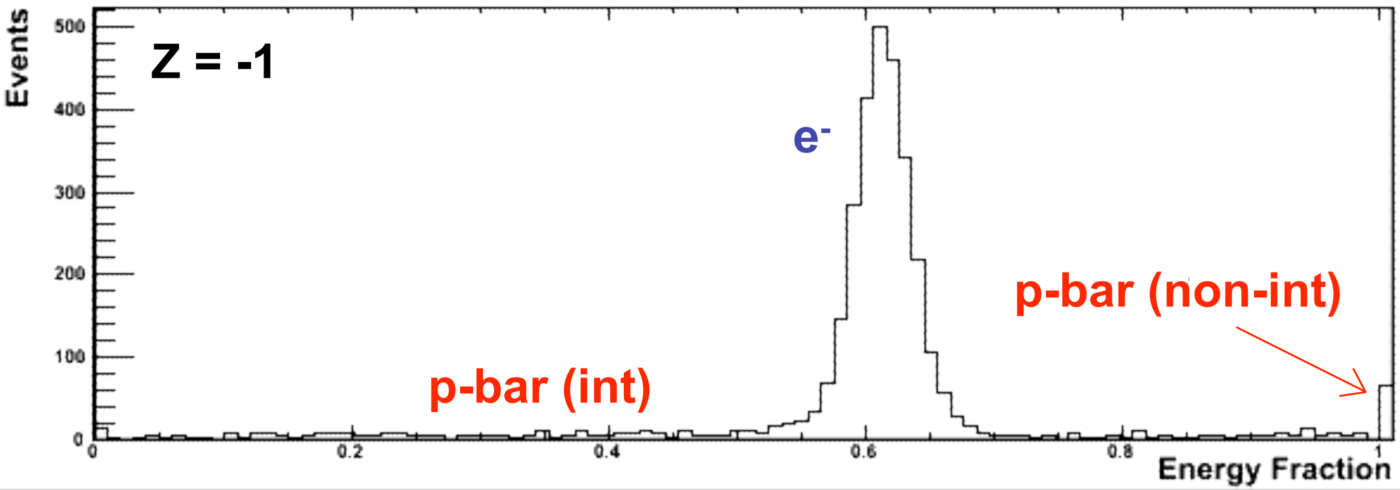

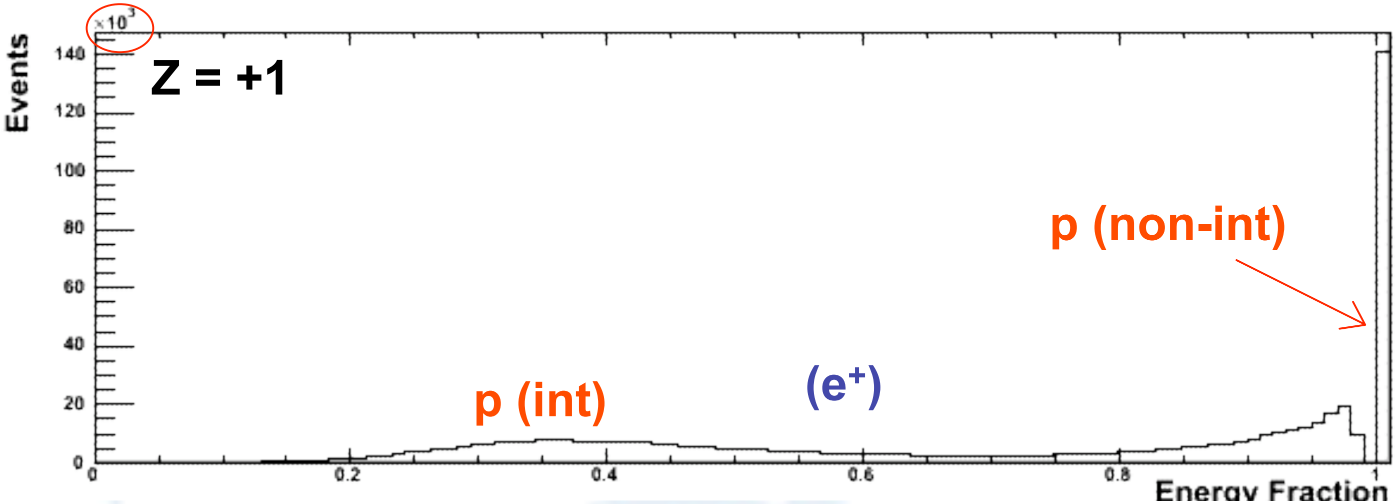

Cut on "energy-rigidity match"

- **Consider the ratio between *total* energy measured by CALO and rigidity measured by TRK.**
  - **For electrons (positrons) ratio is constant over rigidity.**

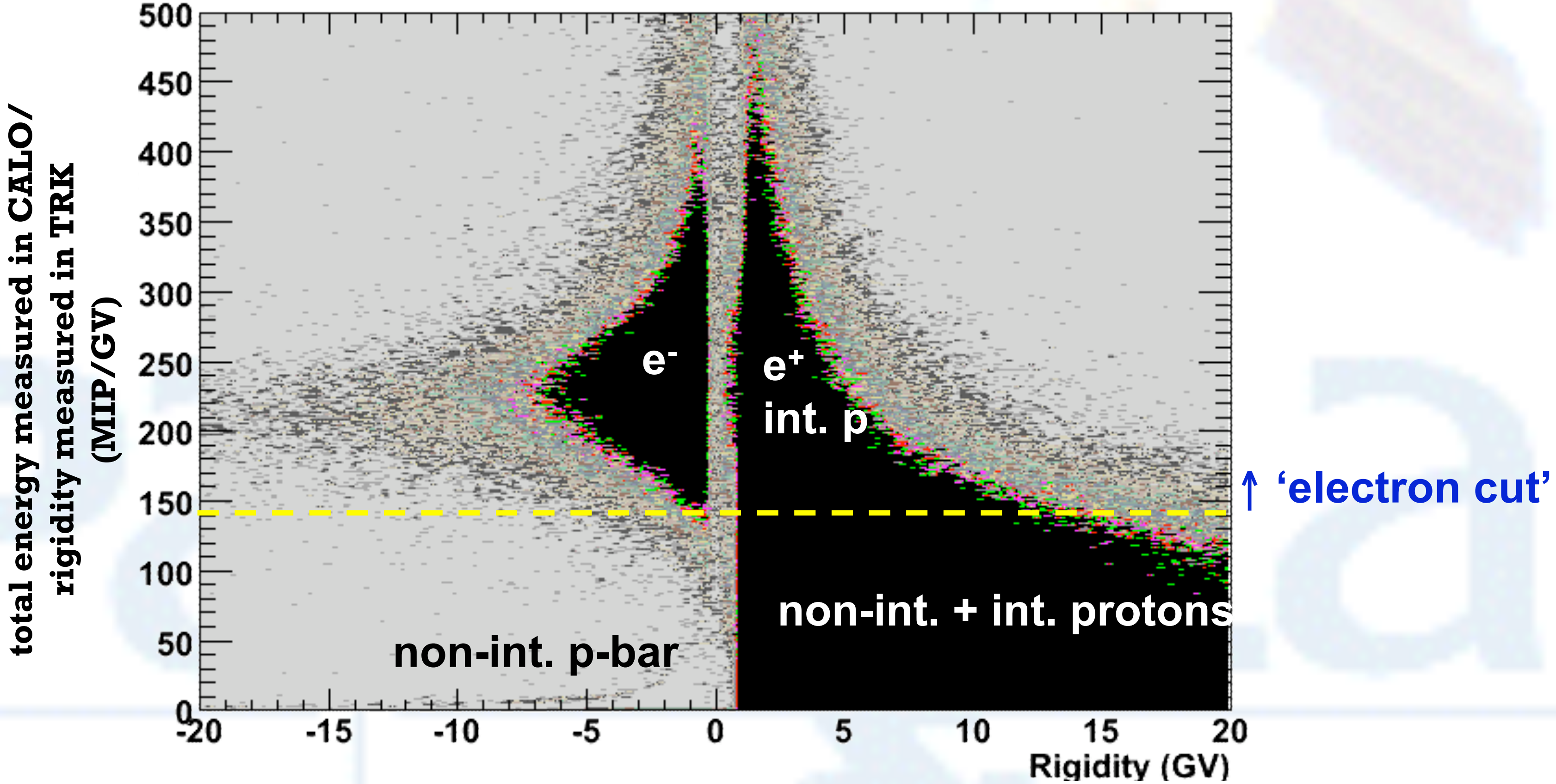

Cut on "energy-rigidity match"

Rigidity: 20-30 GV

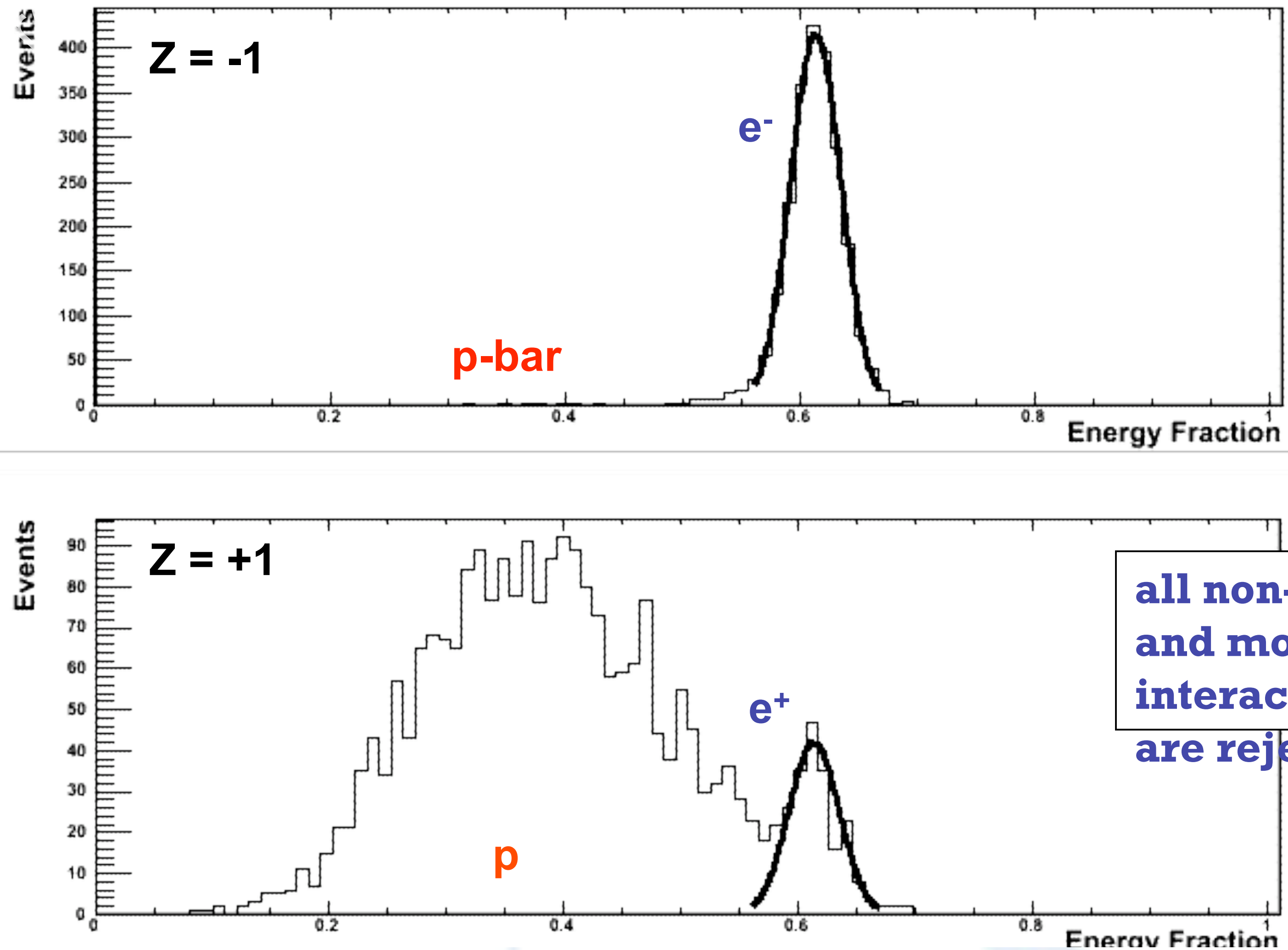

Fraction *F* of energy released in CALO along the track

\+

Constraints on:

Energy-rigidity match

all non-interacting and most interacting protons are rejected

Cut on shower starting point

Constraints on:

Energy-rigidity match

Shower starting point

Flight data.
Rigidity: 20-30 GV

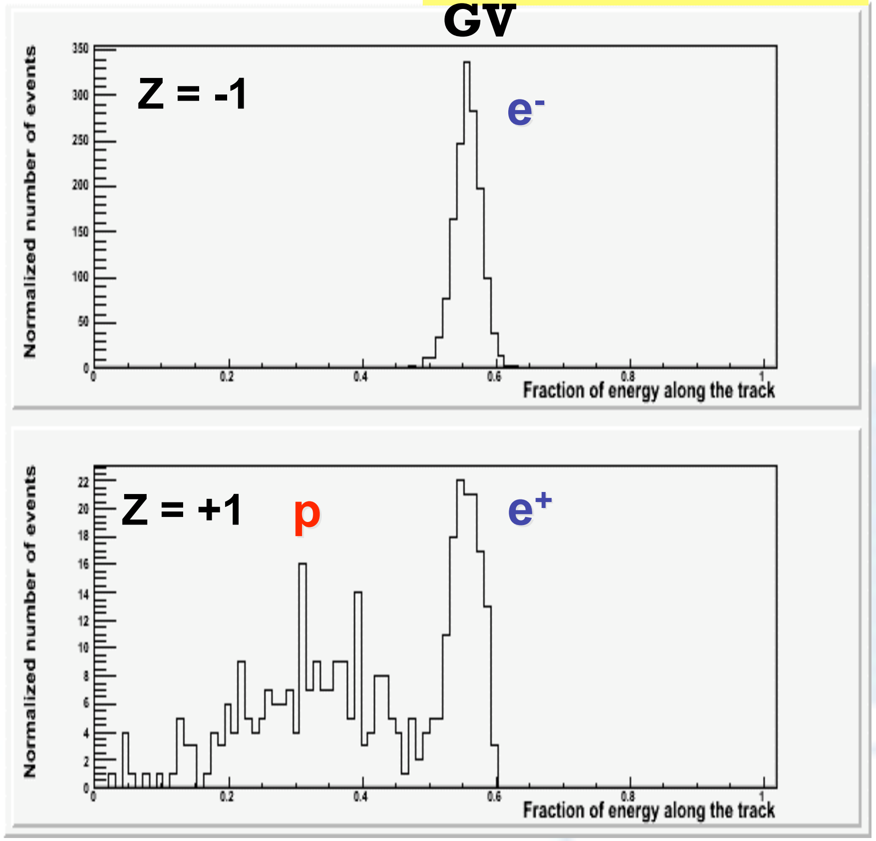

- **Proton background was also characterized at beam tests.**

Beam-test data after same cuts are applie
Rigidity: 50 GV

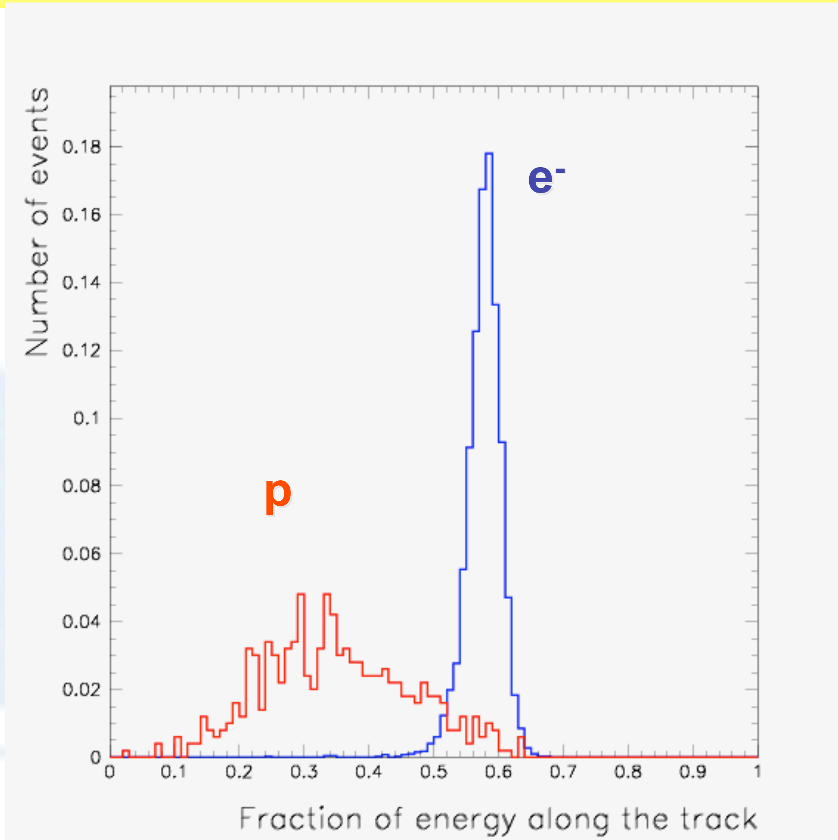

Selected sample after previous cuts

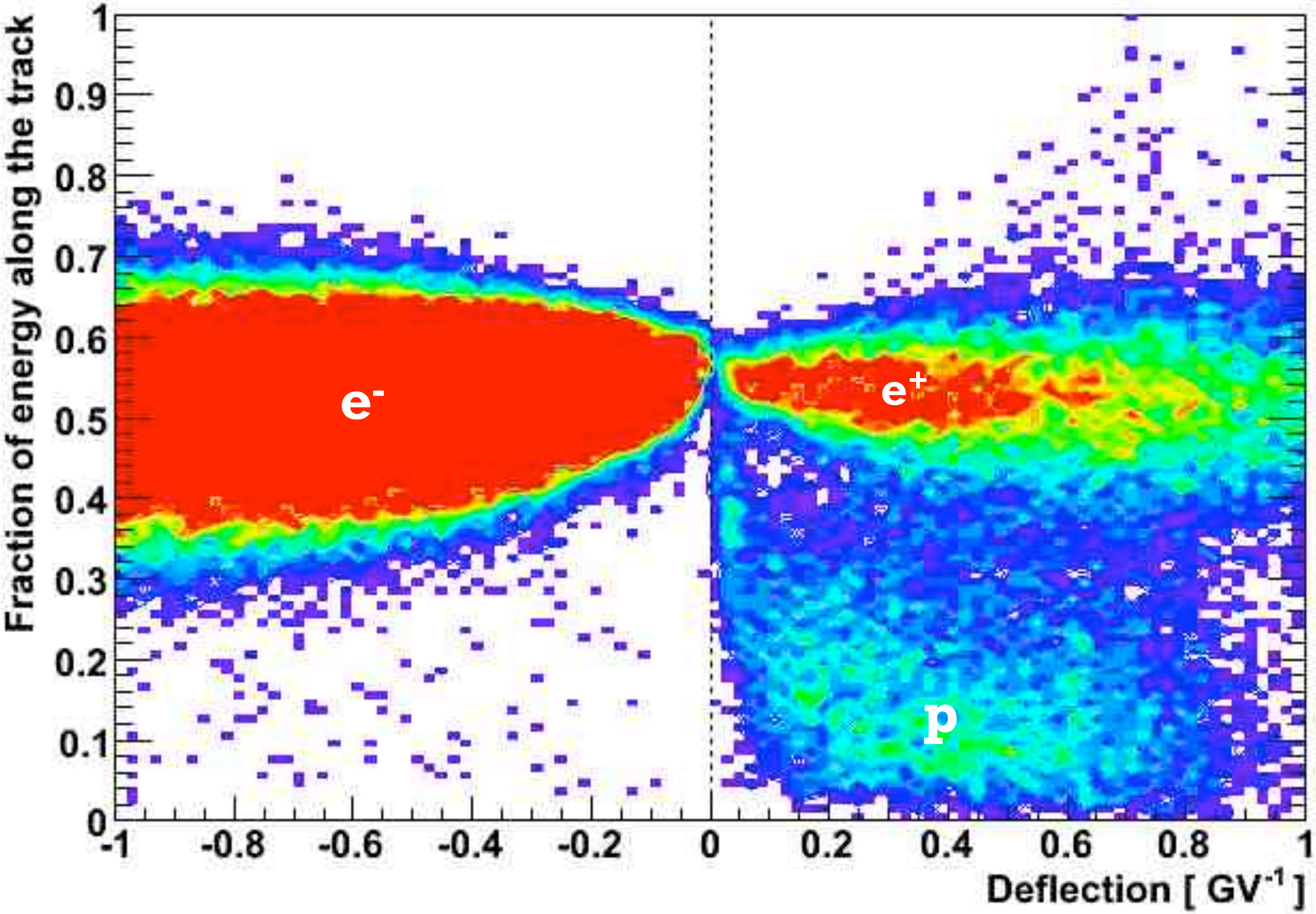

Cross-check: ND flight data

- **Cross-check with flight data from neutron detector to validate the selection procedure.**

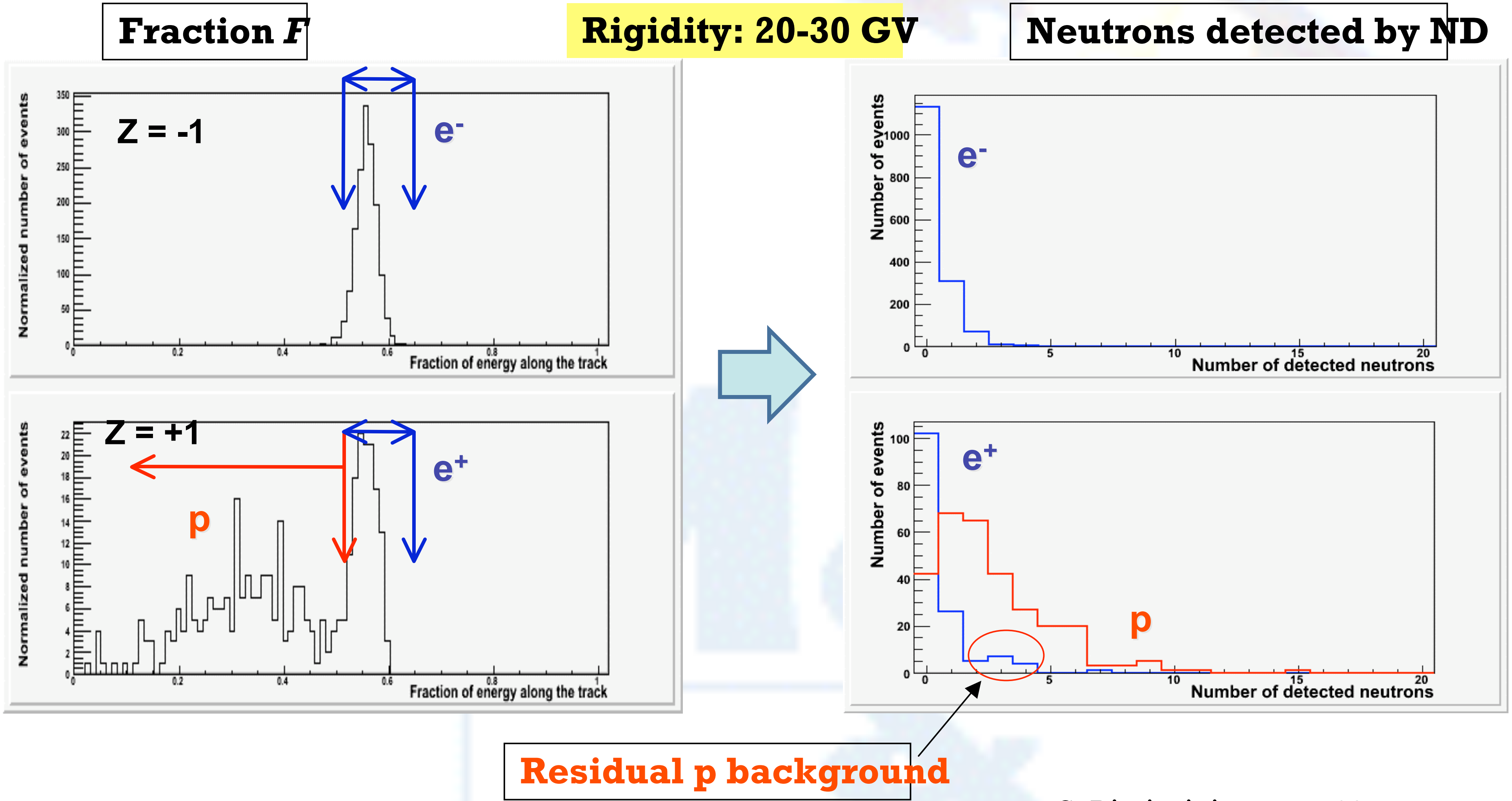

Cut on longitudinal shower profile

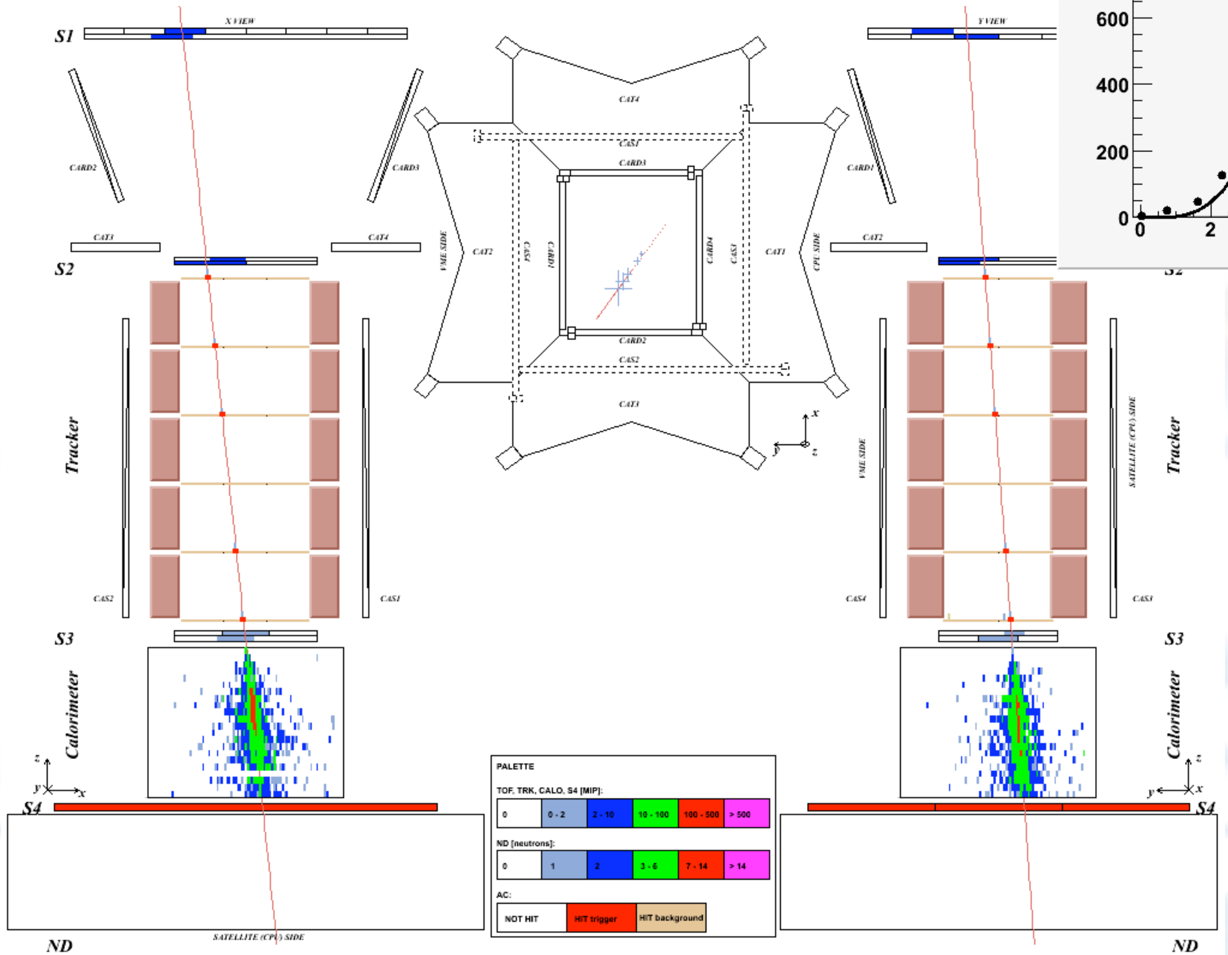

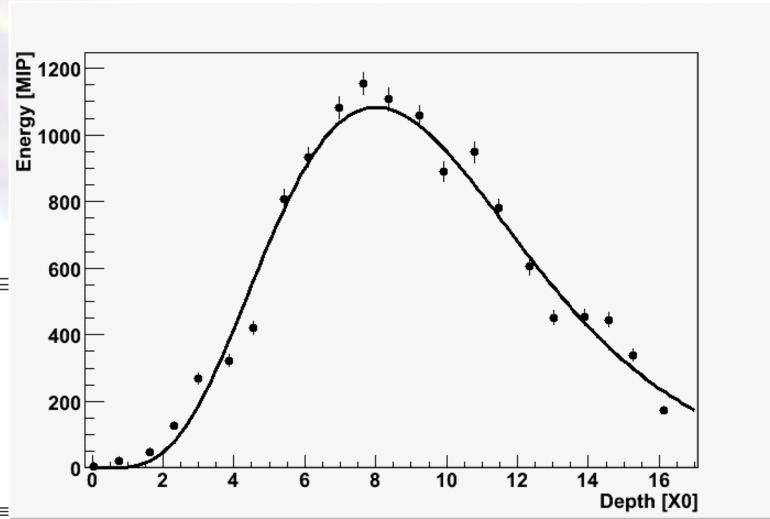

Flight data:
51 GV positron

Cut on longitudinal shower profile

Rigidity: 20-30 GV

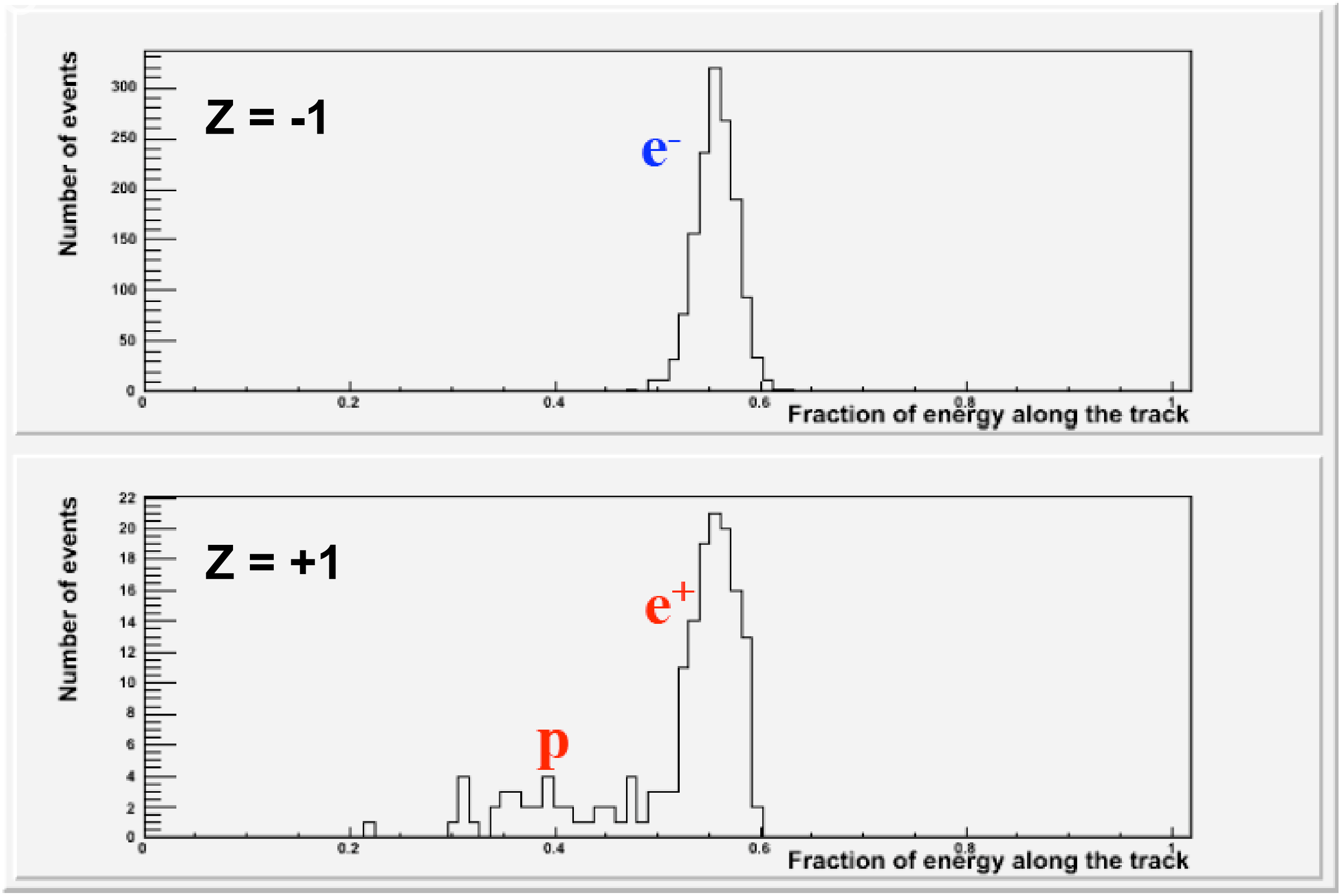

Fraction *F* of energy released in CALO along the track

+

Constraints on:

Energy-rigidity match

Shower starting point

Longitudinal profile

- **Less than 1 proton out of 10^5 survives the complete set of CALO cuts, with e^+ selection efficiency 80%.**

Cross-check: energy loss in TRK

$$-\frac{dE}{dx} = K z^2 \frac{Z}{A} \frac{1}{\beta^2} \left[\frac{1}{2} \ln \frac{2 m_e c^2 \beta^2 \gamma^2 T_{\max}}{I^2} - \beta^2 - \frac{\delta(\beta\gamma)}{2} \right]$$

- **Top: proton and electron samples, identified with TRK only (charge sign).**

Rigidity: 10-15 GV

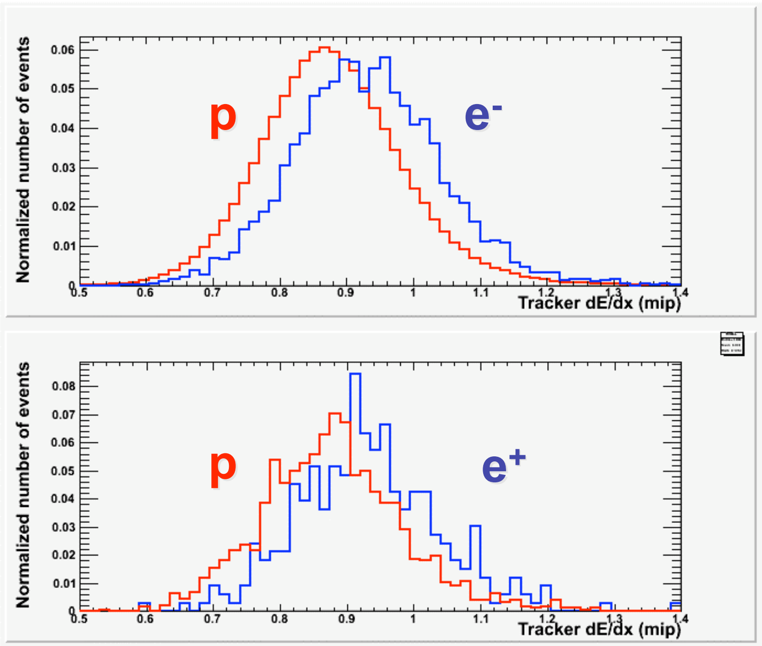

Rigidity: 15-20 GV

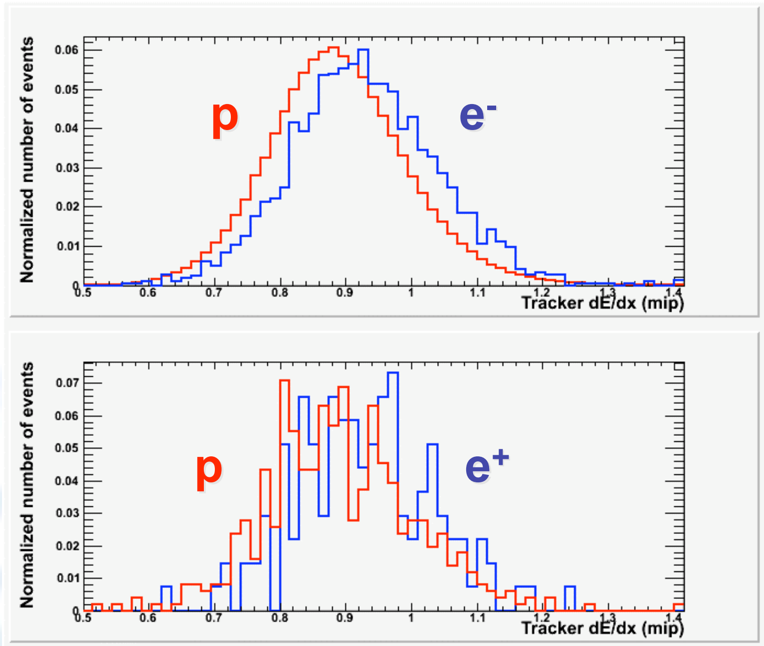

- **Bottom: proton and positron (+ residual p background) samples, identified with present CALO requirements.**

(Step II) Evaluation of residual p background

- **Proton contamination obtained directly from flight data and subtracted with statistical "bootstrap" analysis (no simulation involved).**
  - **Two *reduced*, completely equivalent, CALO geometries are used to characterize the F distribution for positron and proton after all CALO cuts are applied.**

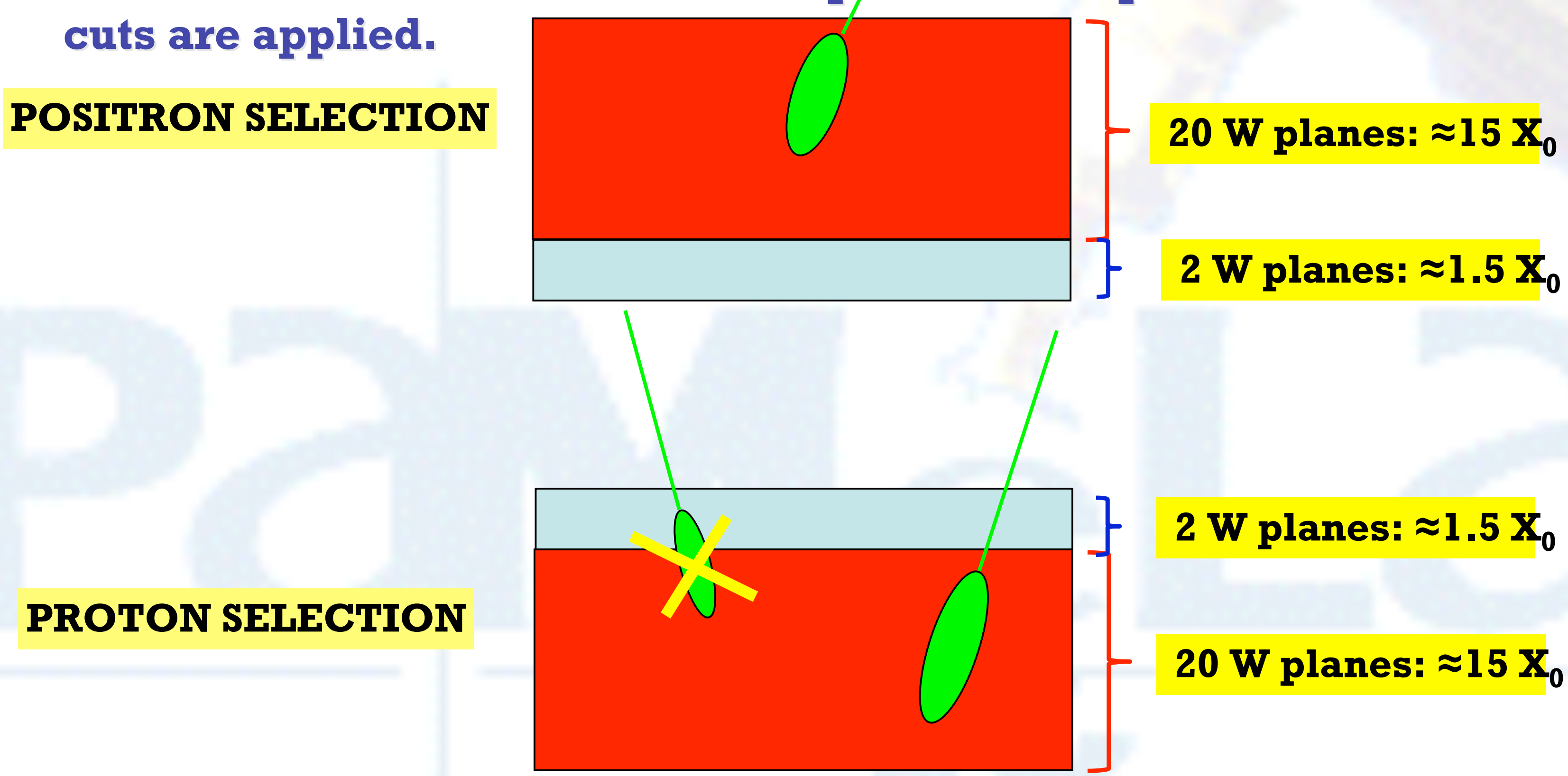

Evaluation of residual p background

Considered three F distributions in *reduced calorimeter* after applying all CALO cuts:

(a) e^- selected in upper CALO.

(b) protons "pre-sampled" in first 2 modules, then selected in lower CALO.

(c) e^+ with residual p background, selected in upper CALO.

Samples (a) and (b) are used to estimate and subtract the proton contamination.

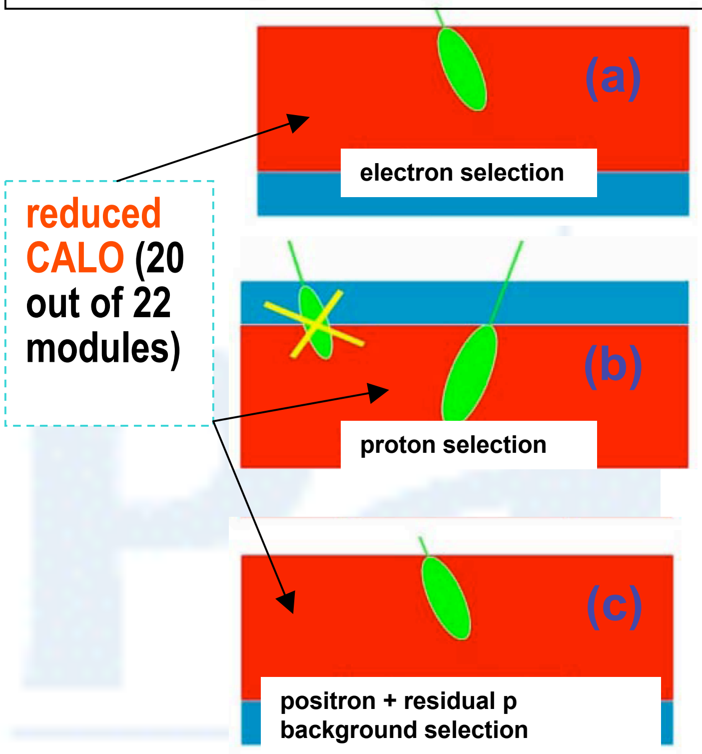

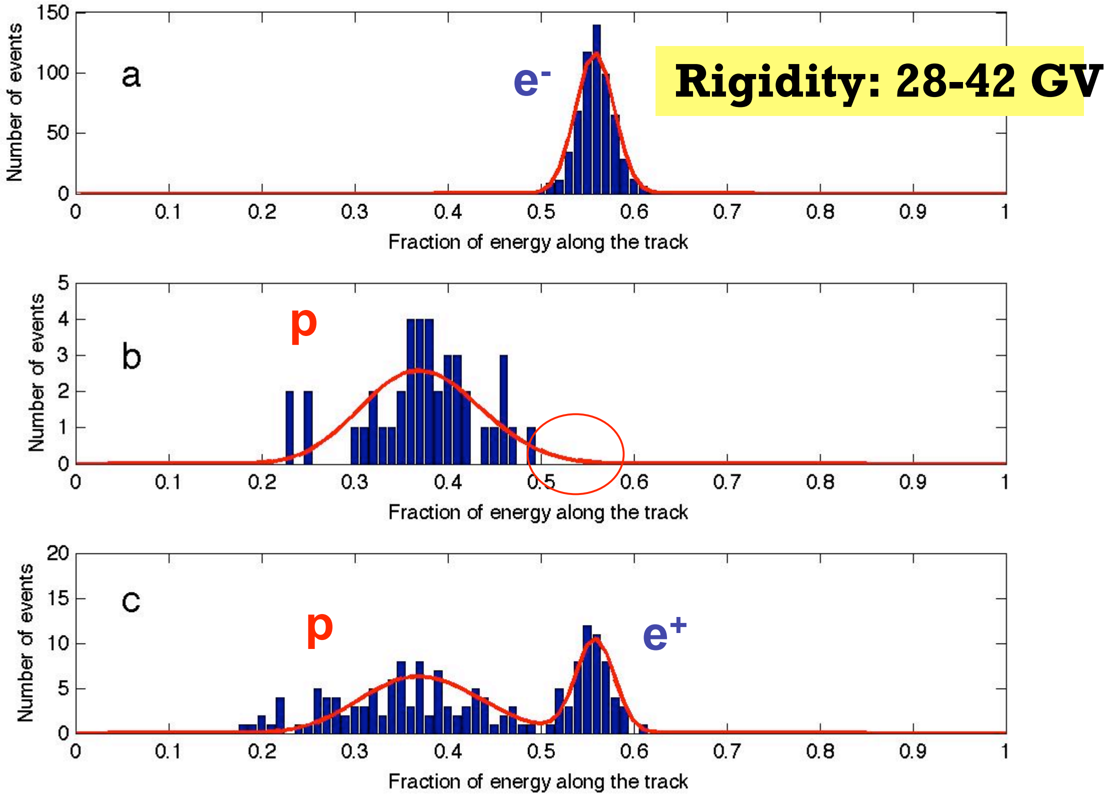

Positron fraction (Nature 458, 2009)

- **One order of magnitude improvement in statistics over previous measurements.**
- **Most extended energy range ever achieved.**
- **Expected further improvements with new data.**

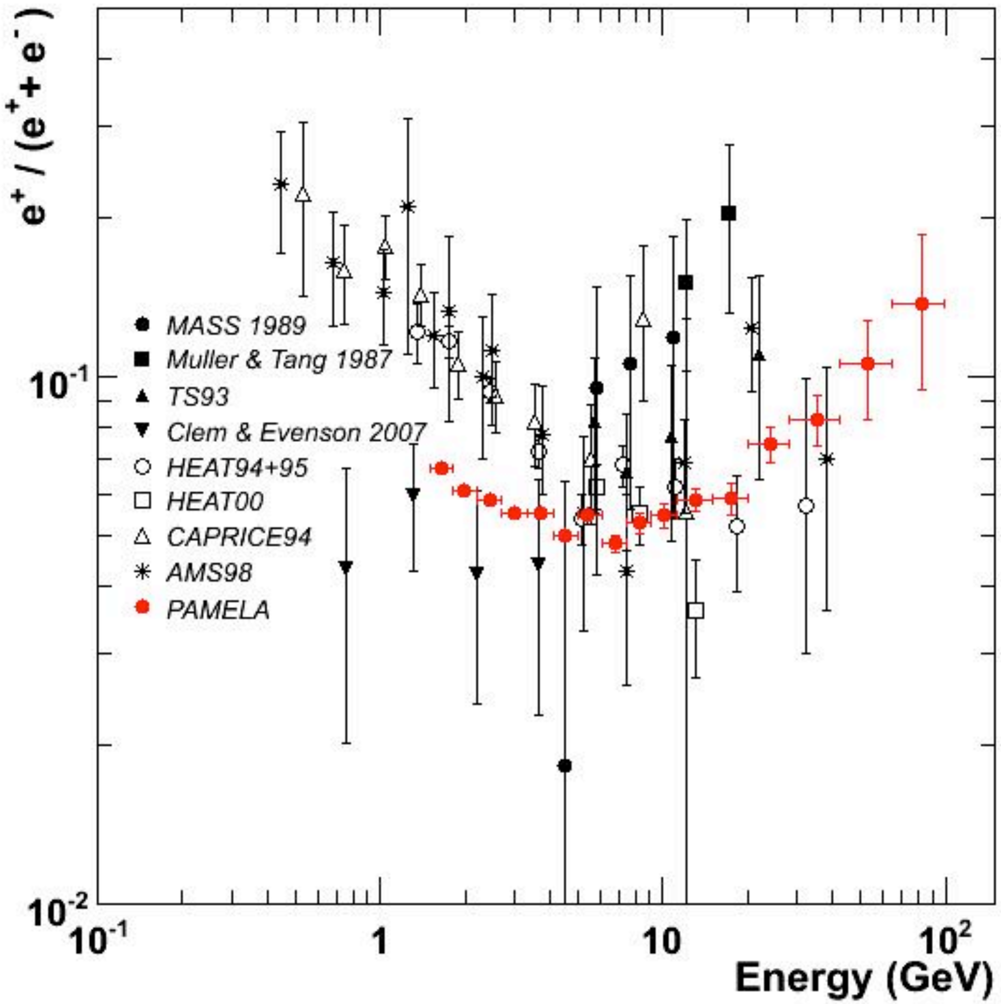

Positron fraction at high energies

- **At high energies our data show a significant increase with energy.**
- **This cannot be explained by standard models of secondary production of cosmic rays.**
  - Either a significant change in the acceleration or propagation models is needed;
  - or a primary component is present.
- **Among primary-component candidates:**
  - annihilation of dark matter in the vicinity of our galaxy;
  - near-by astrophysical sources,

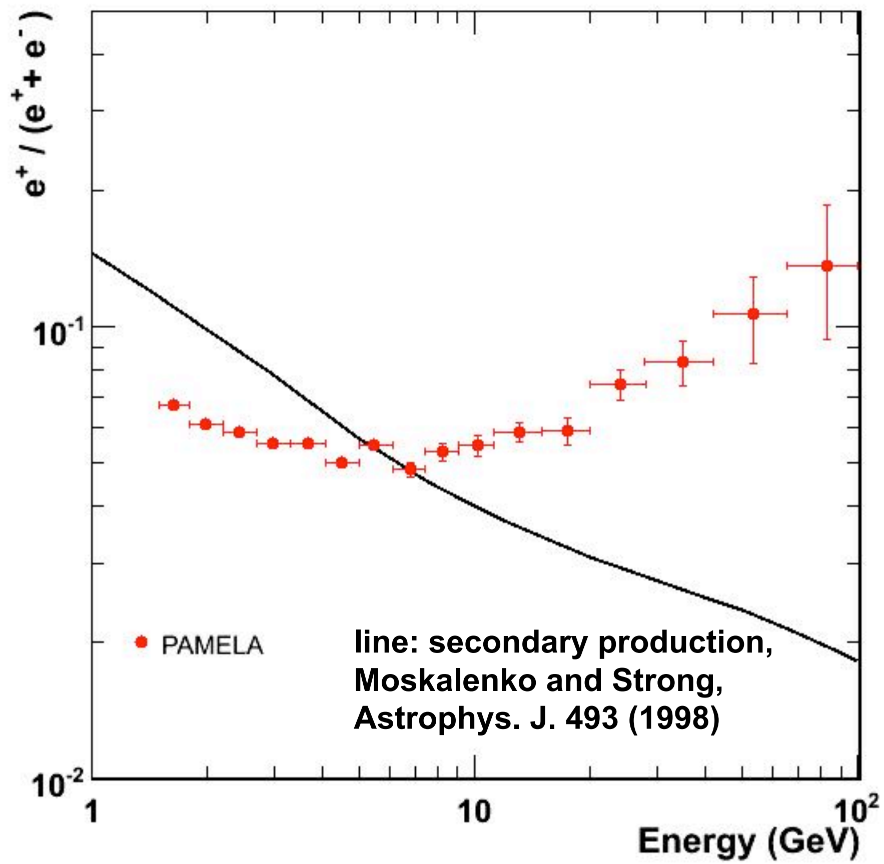

Positron fraction at low energies

- **At low energies our results are systematically lower than data collected in 1990's.**
  - **Clem 2007 (with much lower statistics) is consistent with PAMELA.**
- **This is interpreted as effect of charge-sign dependent solar modulation.**
  - **our data are enough precise to allow tuning of models of the heliosphere.**
- **Ruled out as negligible a possible combined effect of:**
  - **asymmetry of spectrometer magnetic field;**
  - **East-West effect or reentrant albedo particles.**

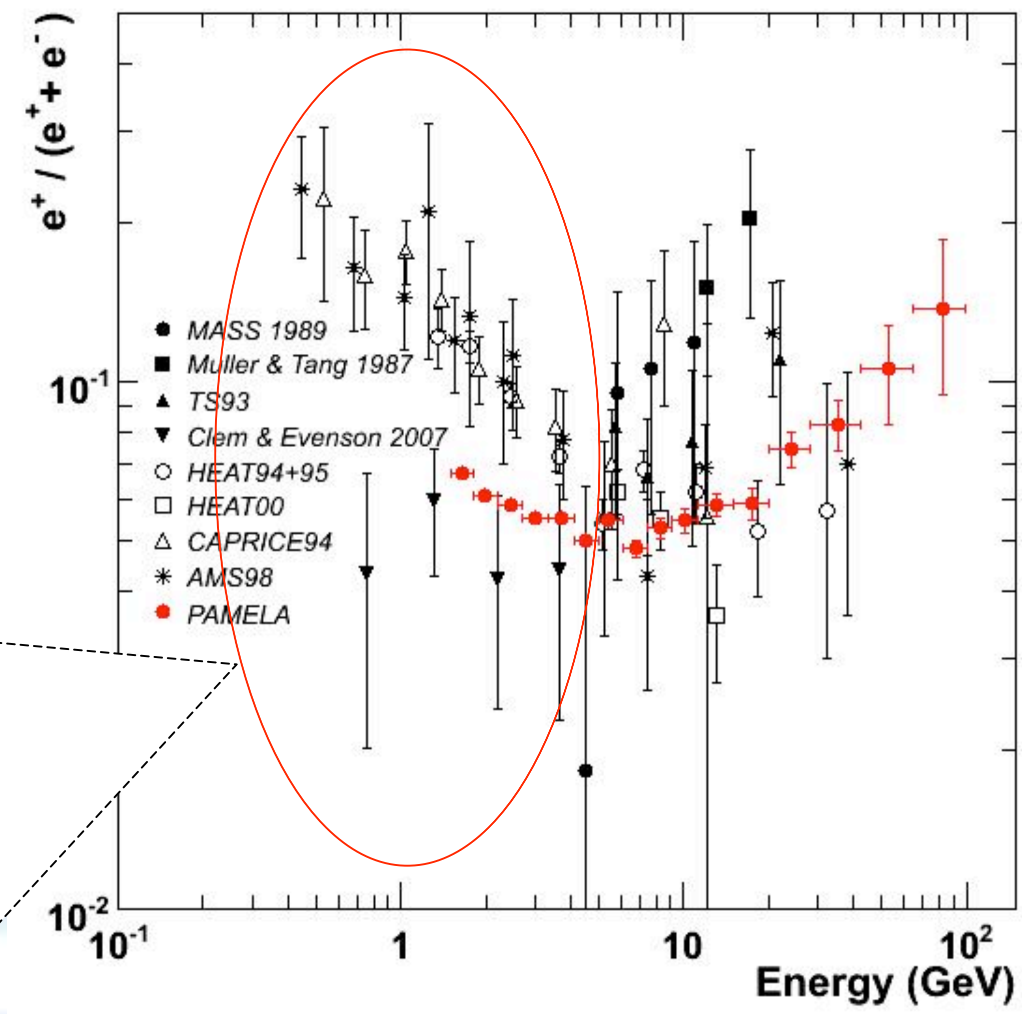

(3) Measurement of absolute differential fluxes

Absolute flux and selection efficiencies

- **Measurement of absolute differential flux requires the evaluation of several additional factors:**

$$J(bin) = \frac{N_{SEL}}{T_{LIVE}} \cdot \frac{1}{\varepsilon_{TRIG}} \cdot \frac{1}{\varepsilon_{SEL}} \cdot \frac{1}{E_{\max} - E_{\min}} \cdot \frac{1}{G}$$

- **Specifically, the evaluation of ε_{SEL}, if not properly addressed, can introduce systematic errors, whose weight can be greater than residual contamination background:**
  - **possible energy-dependent bias in ε_{SEL} can alter the flux spectral index.**

- **Protons, given the high statistics and low background contamination, can be used to define optimized methodologies:**
  - **for the direct measurement of ε_{SEL} with experimental data;**
  - **aiming at reducing the overall systematic error ε_{SEL} to the order of few %.**

PAMELA geometric factor G

- **G defined to include only effect of instrument geometry and magnetic field.**
  - **interactions are taken into account as a further (generally small) simulated correction.**

- **With such method:**
  - **G(R) depends only on rigidity;**
  - **a very precise (deterministic) numerical approximation technique has been developed in addition to usual Monte Carlo technique;**
  - **overall calculation error < 0.5% at high energies.**

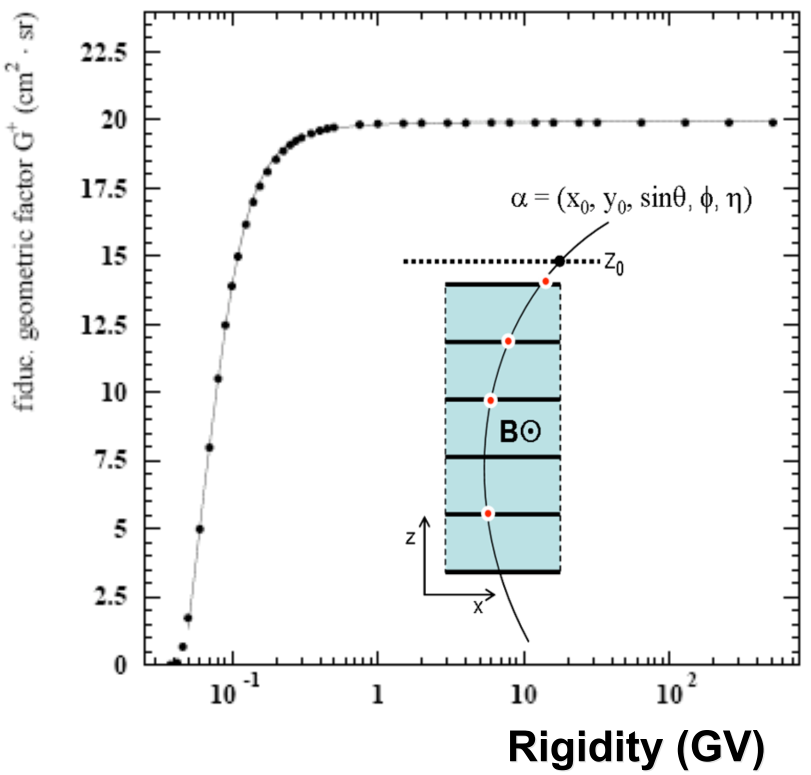

- **Defined a fiducial 92% volume to avoid systematics at acceptance borders from mechanical**

(3.a) Proton absolute flux

General approach for p flux

- **Given the absence of high-statistic sources of contamination in the proton sample, a set of standard cuts is sufficient to reject all unwanted events:**
  - **clean event pattern (ANTI, TOF);**
  - **minimal track requirement for good rigidity measurement;**
  - **galactic particle (downward, above cutoff);**
  - **|Z|=1 from dE/dL vs. R.**
  - **loose MDR cut: MDR > R_{max}(bin).**

- **Selection with CALO is not necessary:**
  - **negligible positron contamination.**

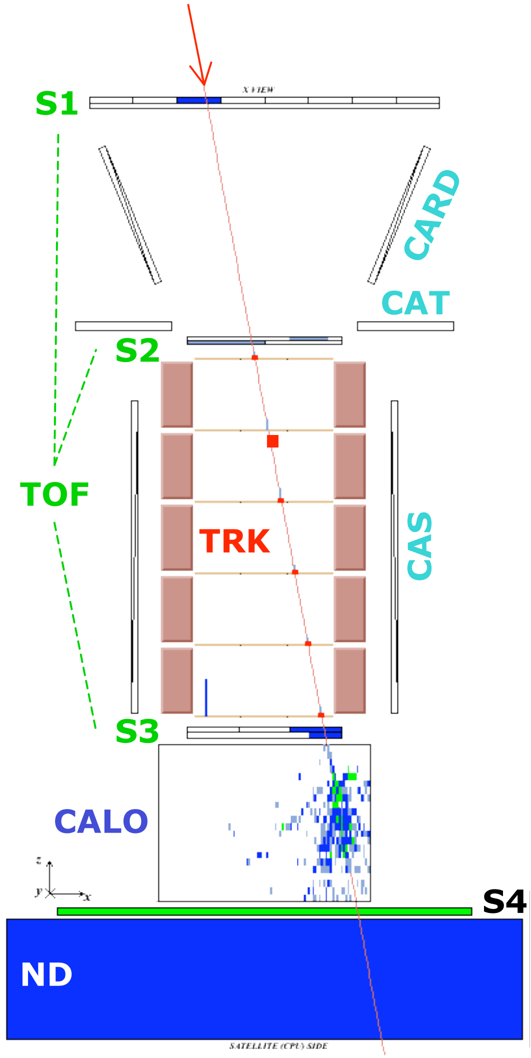

Measurement of selection efficiency

- **Selection efficiency $\varepsilon_{SEL}(R)$ experimentally measured with flight data.**

- **Main effort to select as much as possible clean and unbiased samples.**
- **In particular, reduce and correct possible "sample distortion" effects:**
  - **the distribution of energy and of incidence point and direction of the protons in the efficiency sample can be different with respect to the ideal required one;**
  - **if coupled to a corresponding non-homogeneity of the measured efficiency, this can introduce a significant bias in the measured efficiency.**

- **Simulation used to cross-check experimental efficiencies and to apply second-order corrections for residual biases.**

- **Results derived with proton analysis are applied to the other, less**

Measurement of selection efficiency

- ε_{SEL} operatively defined as the product of relative efficiencies (i.e. conditioned probabilities) corresponding to several sets of cuts:
  - (1) TRK basic: single track, no other requirements
  - (2) TOF: $\beta>0$ and pattern consistent with single TRK track
  - (3) TRK minimal requirements (hits + χ^2)
  - (4) no activity in CAT+CARD (anticoincidence)
  - (5) $|Z|=1$ from dE/dL vs. R
  - (6) TRK MDR > R_{max}(bin)

$$\varepsilon_{SEL} = \varepsilon_{TRK\_basic} \cdot \varepsilon_{TOF} \cdot \varepsilon_{TRK\_hit+\chi^2} \cdot \varepsilon_{ANTI} \cdot \varepsilon_{TRK\_dE/dL} \cdot \varepsilon_{TRK\_MDR}$$

- Each efficiency is independently, experimentally measured;
  - by defining relative efficiencies, *correlations* between different sets are automatically taken into account.

Efficiency of TRK basic cut

- It is derived by selecting a proton sample with TOF, ANTI and CALO.
  - Particle tracks are reconstructed in the calorimeter, back-propagated and required to be inside the fiducial acceptance volume.
  - Trajectories are approximated as straight lines (uncertainty estimated with simulation to be negligible in the rigidity region of interest).
- Below about 1 GeV the particle rigidity is reconstructed by measuring the velocity with the TOF and assuming a proton mass.
  - Above such threshold no independent rigidity information is available in experimental data.
  - Anyway, from simulation the TRK efficiency does not show any significant variation with rigidity.
- The geometric distribution of this efficiency sample is not perfectly isotropic while the TRK basic efficiency is not uniform over the acceptance range:
  - a corresponding (~1%) correction is derived by simulation.

Preliminary proton spectrum

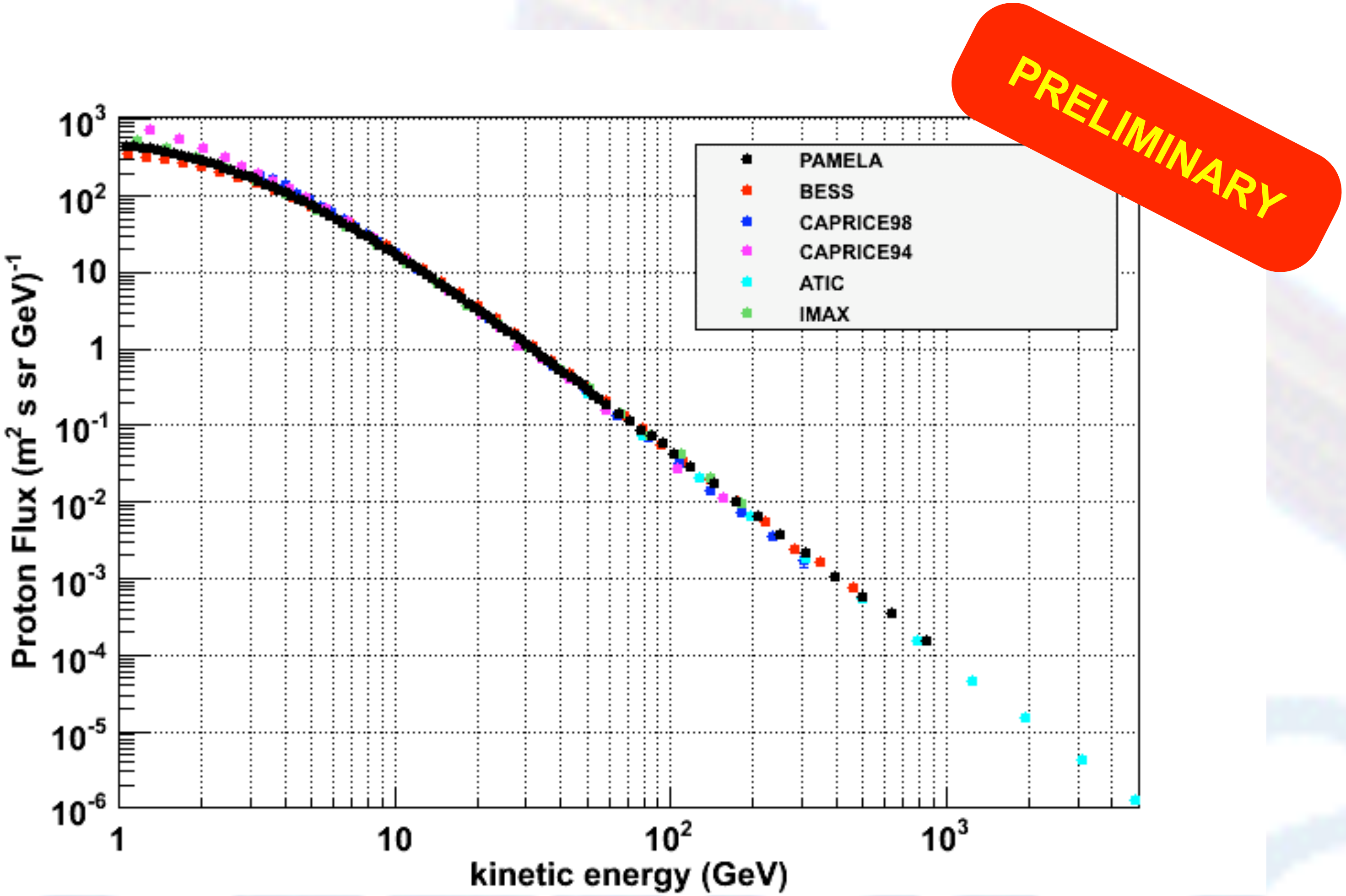

- **Combined corrections from simulations (efficiency biases, particle loss or contamination from interactions) are ~1% above few GeV.**

Preliminary proton spectrum

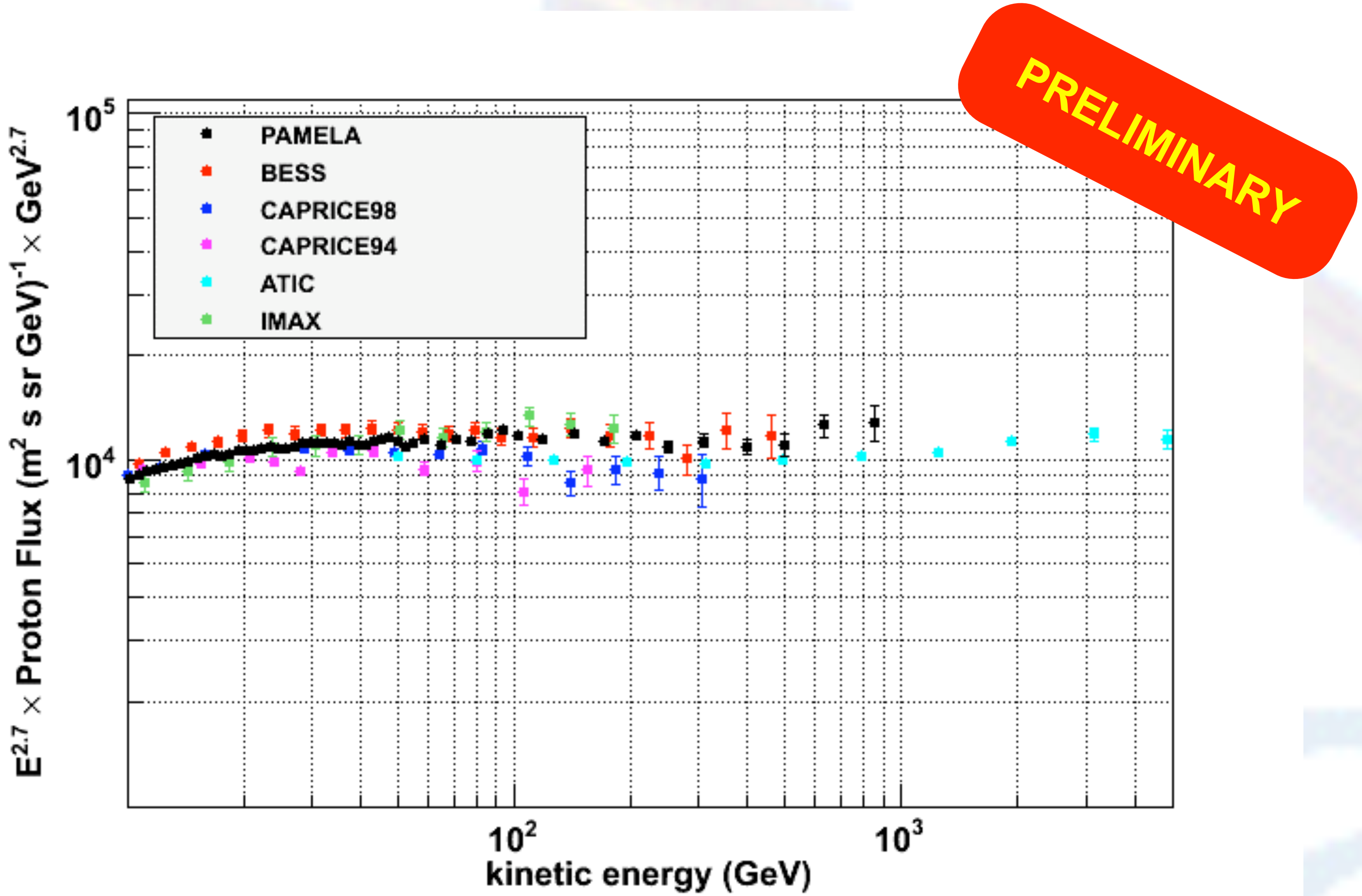

- Upper energy range limited by the uncertainty in TRK rigidity measurement.
  - evaluation of systematic from rigidity uncertainty is under way;
  - it mostly concerns higher rigidity bins ("unfolding" methods under study);

(3.b) Antiproton absolute flux

Antiproton selection criteria

- All proton cuts.
- Additional cuts (as for p-bar/p ratio):
  - electron rejection with CALO;
  - pion rejection at low energies with β vs. R;
  - further track quality requirements to reject "spillover" protons.
- All selection efficiencies evaluated with proton samples:
  - assumed identical response of the apparatus for p and p-bar;
  - correction for hadronic interaction in CALO from simulation.

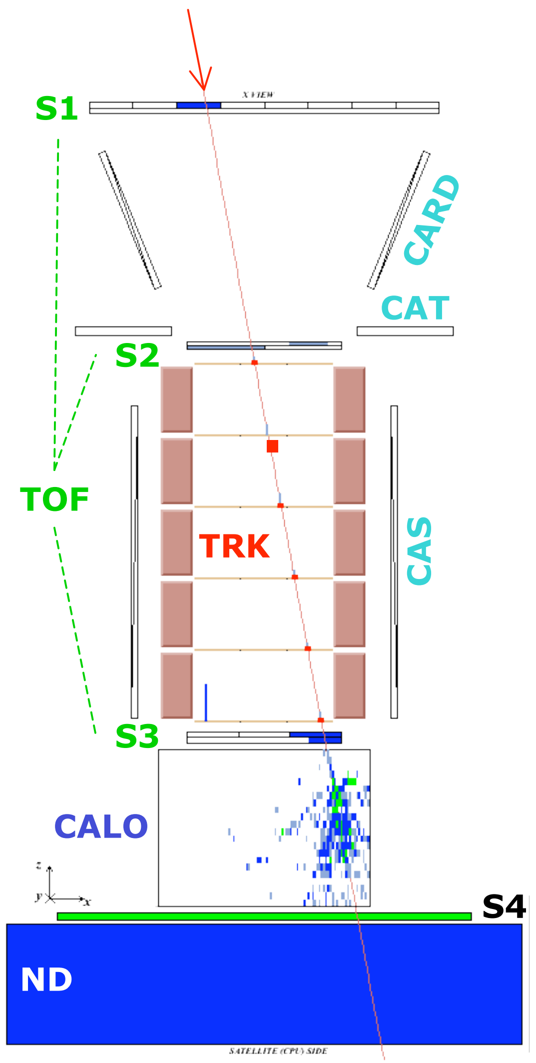

Antiproton selection criteria

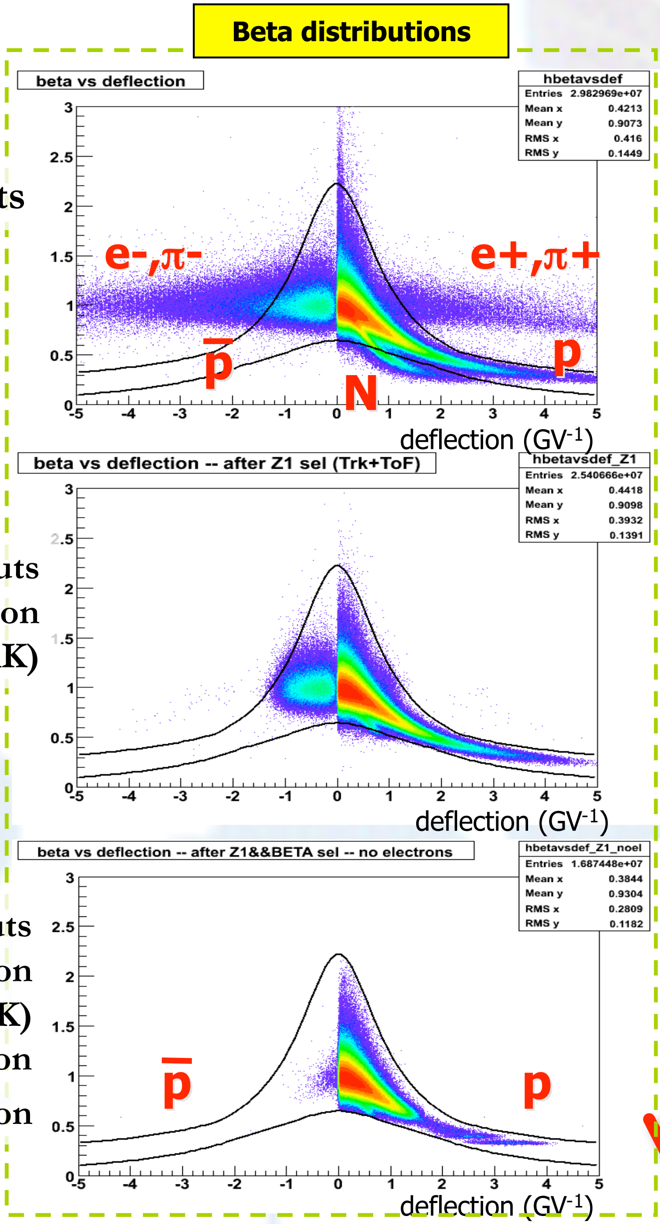

Basic cuts

Basic cuts
+ dE/dL selection
(TOF+TRK)

Basic cuts
+ dE/dL selection
(TOF+TRK)
+ β selection
+ Calo selection

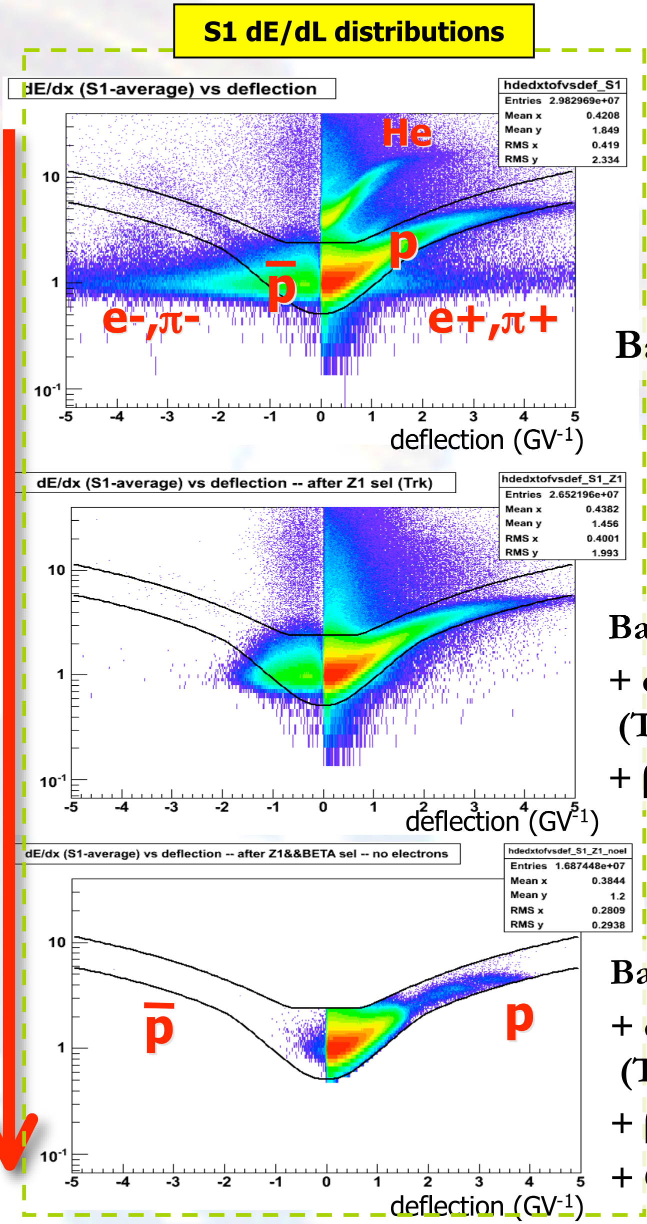

Basic cuts

Basic cuts
+ dE/dL selection
(TRK)
+ β selection

Basic cuts
+ dE/dL selection
(TRK)
+ β selection
+ Calo selection

Residual pion contamination

- **Protons interacting in the material surrounding PAMELA can generate π⁻ which mimic p-bar.**
- **Residual contamination of π⁻ passing selection cuts estimated with extensive and accurate FLUKA2006-based simulation.**
  - **Contamination is ~ 10% at 1 GeV, < 1% above 3 GeV.**

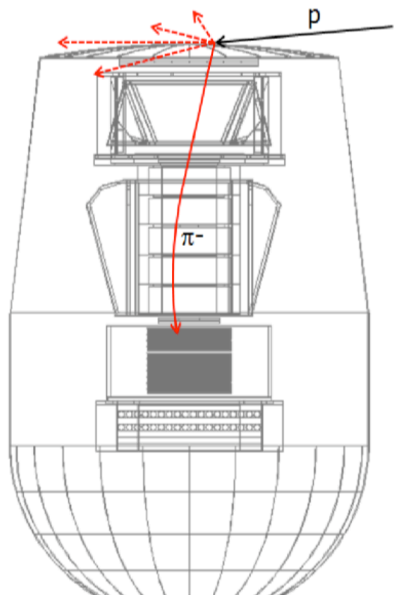

- **Simulation results are validated by comparison with flight data (<1 GV pion sample).**

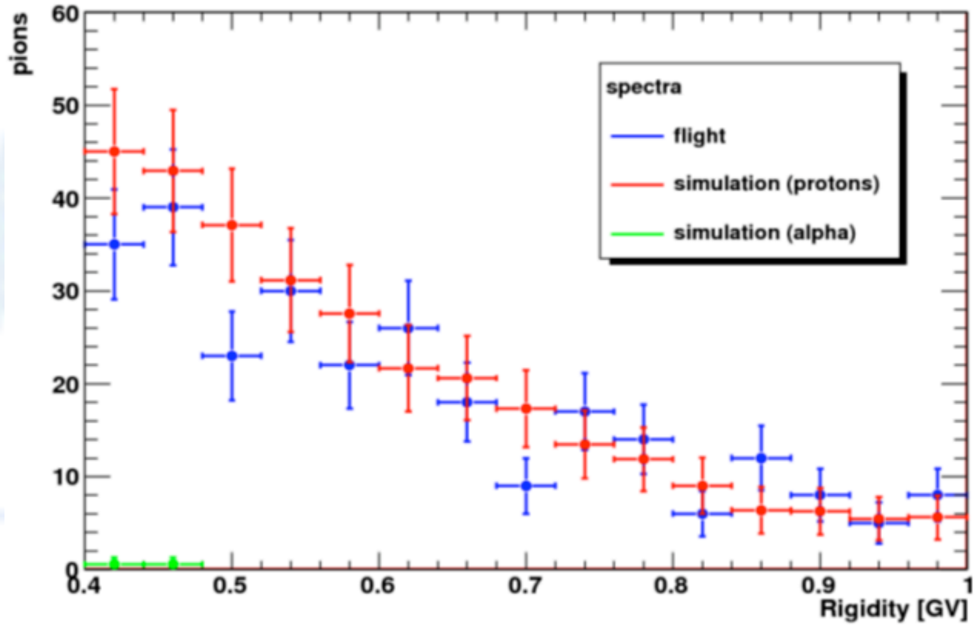

Preliminary p-bar spectrum

- **Evaluation of systematics is under way.**

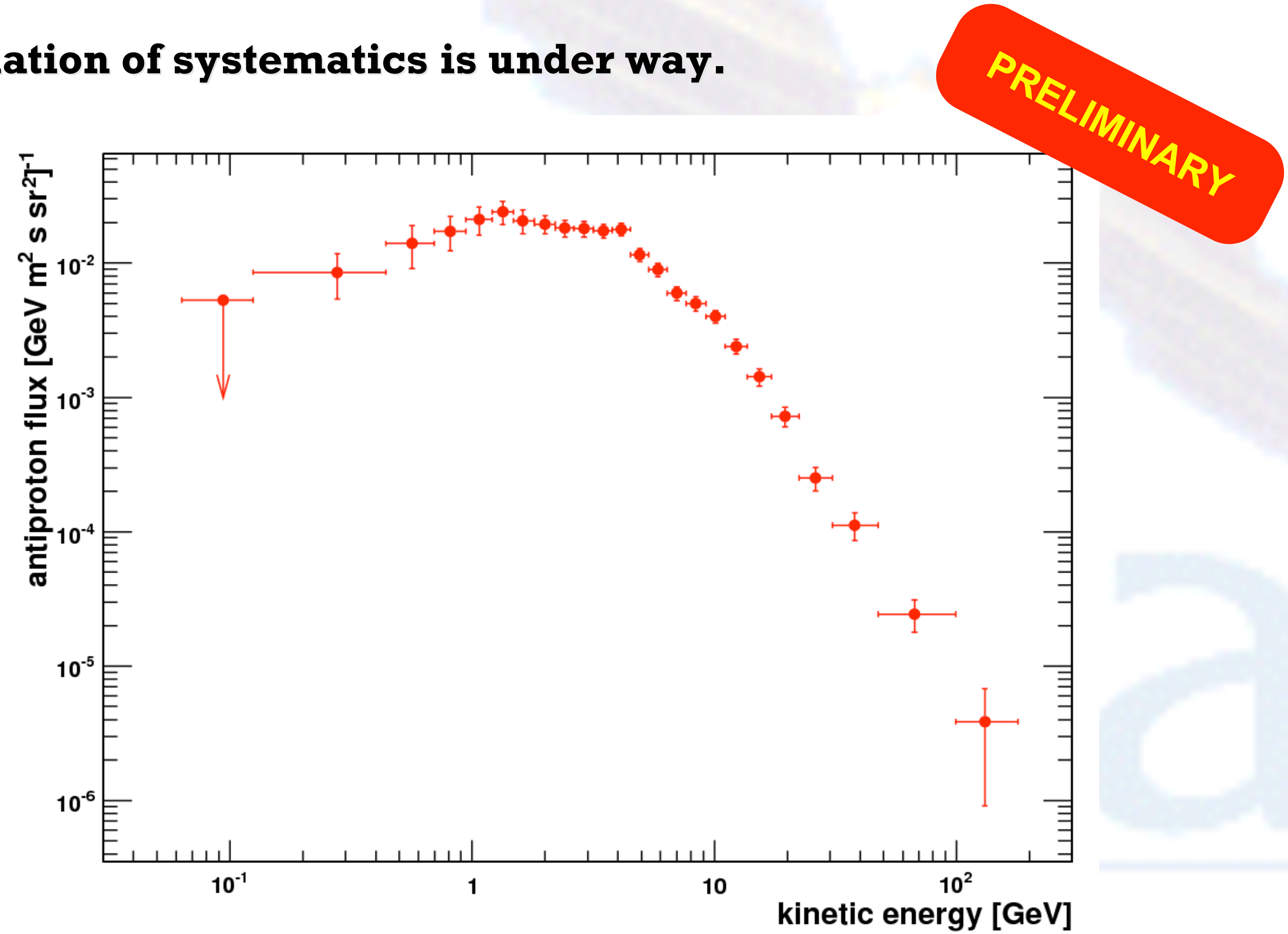

Preliminary p-bar spectrum

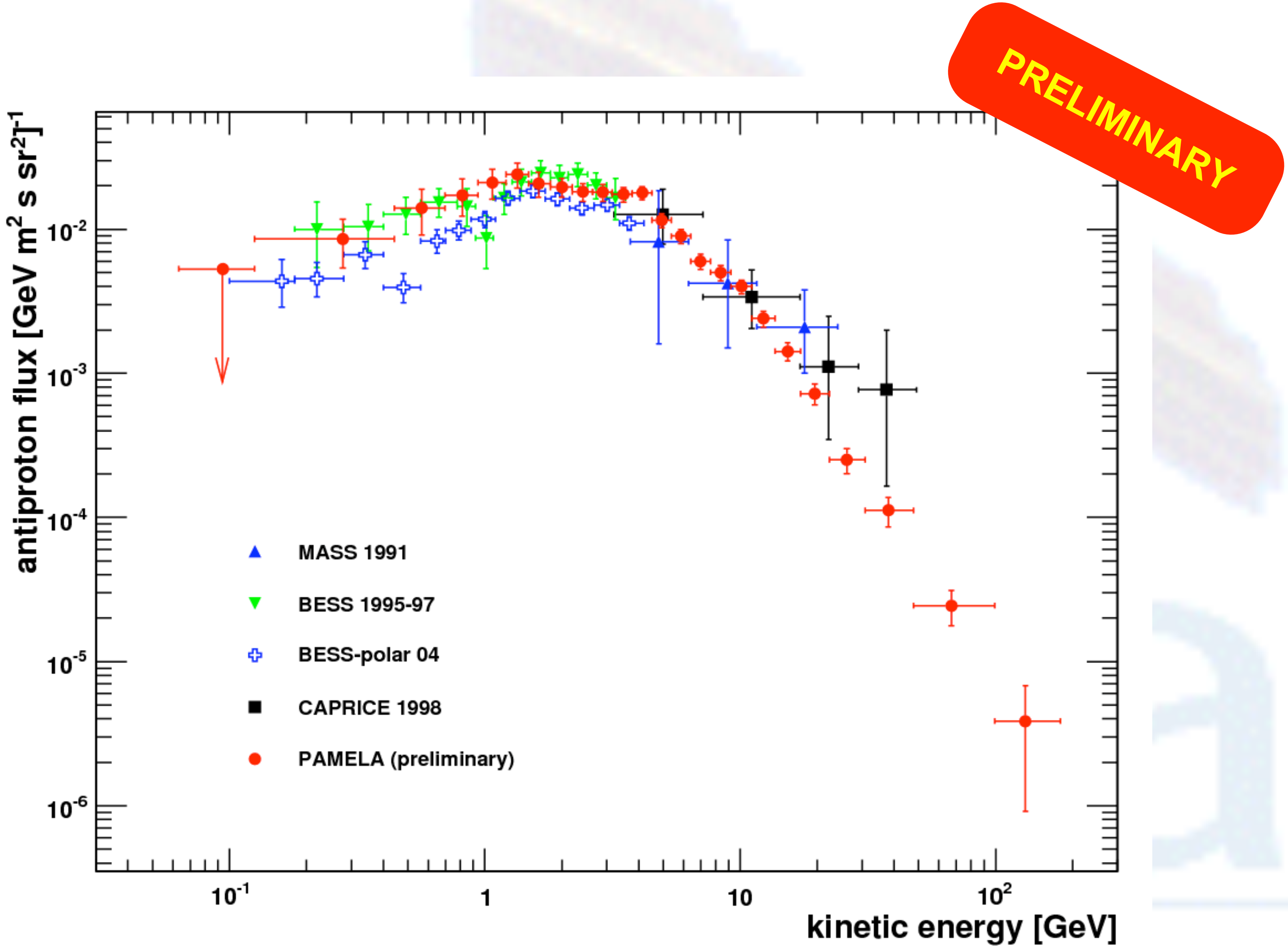

Preliminary p-bar spectrum

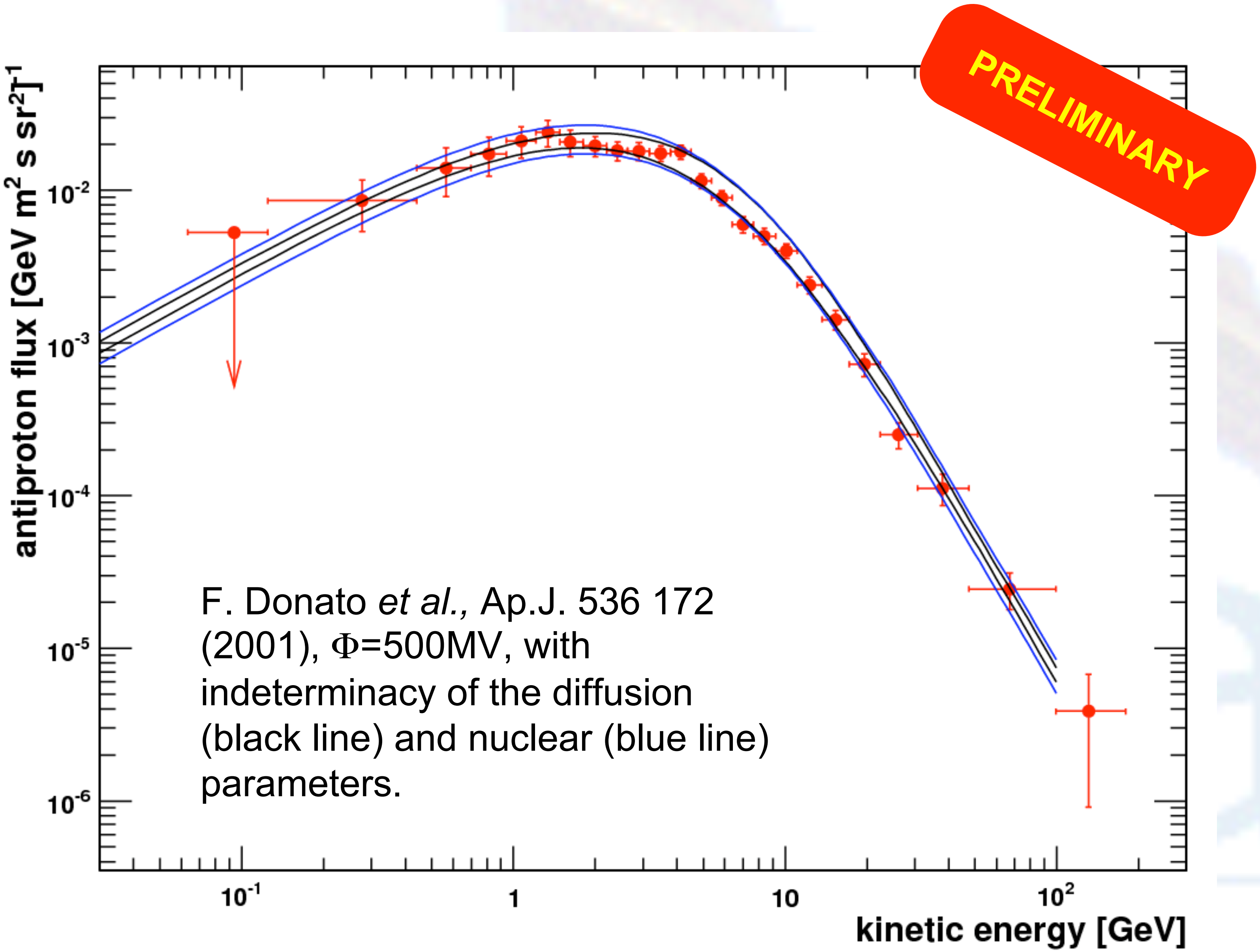

(3.c) Helium absolute flux

Selection of Helium

- **Redundant |Z|=2 identification with independent detectors (TRK, TOF, CALO first plane).**
  - **selection efficiency can then be measured with flight data.**

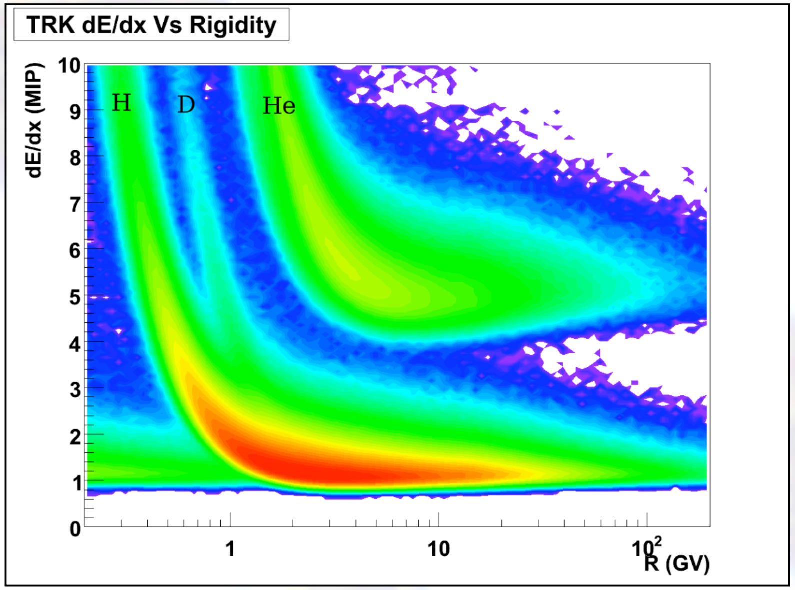

Also: residual contamination from proton after TRK selection can be measured with TOF.

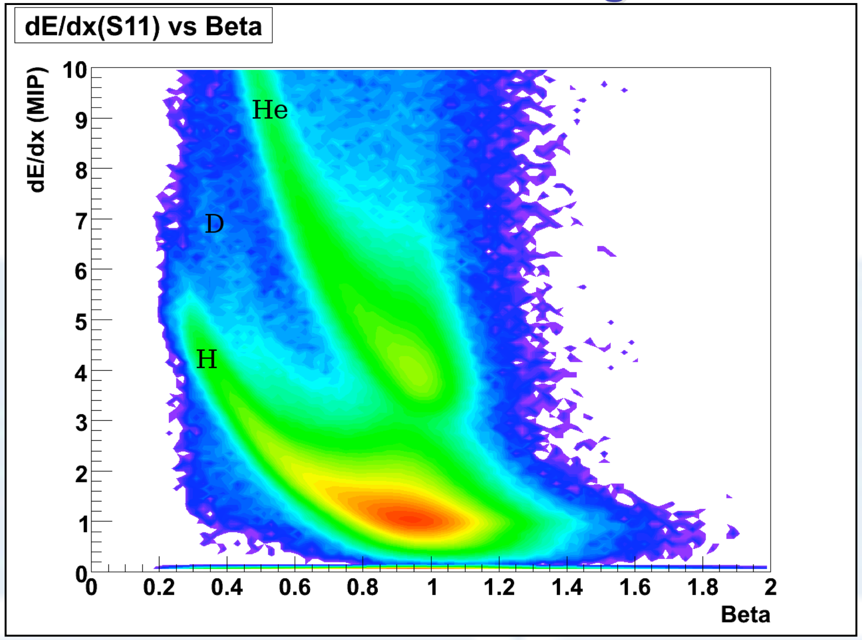

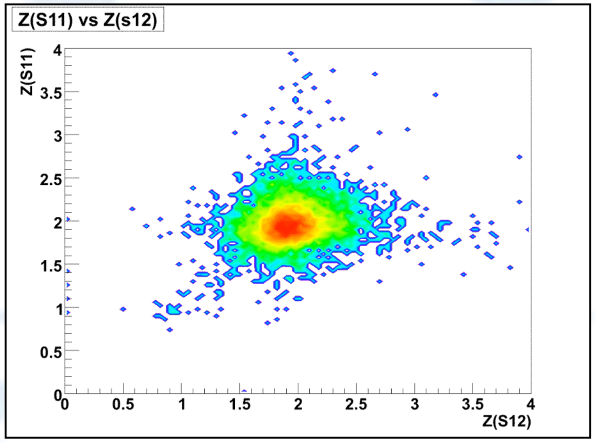

Preliminary He spectrum

- **Evaluation of systematics is under way.**

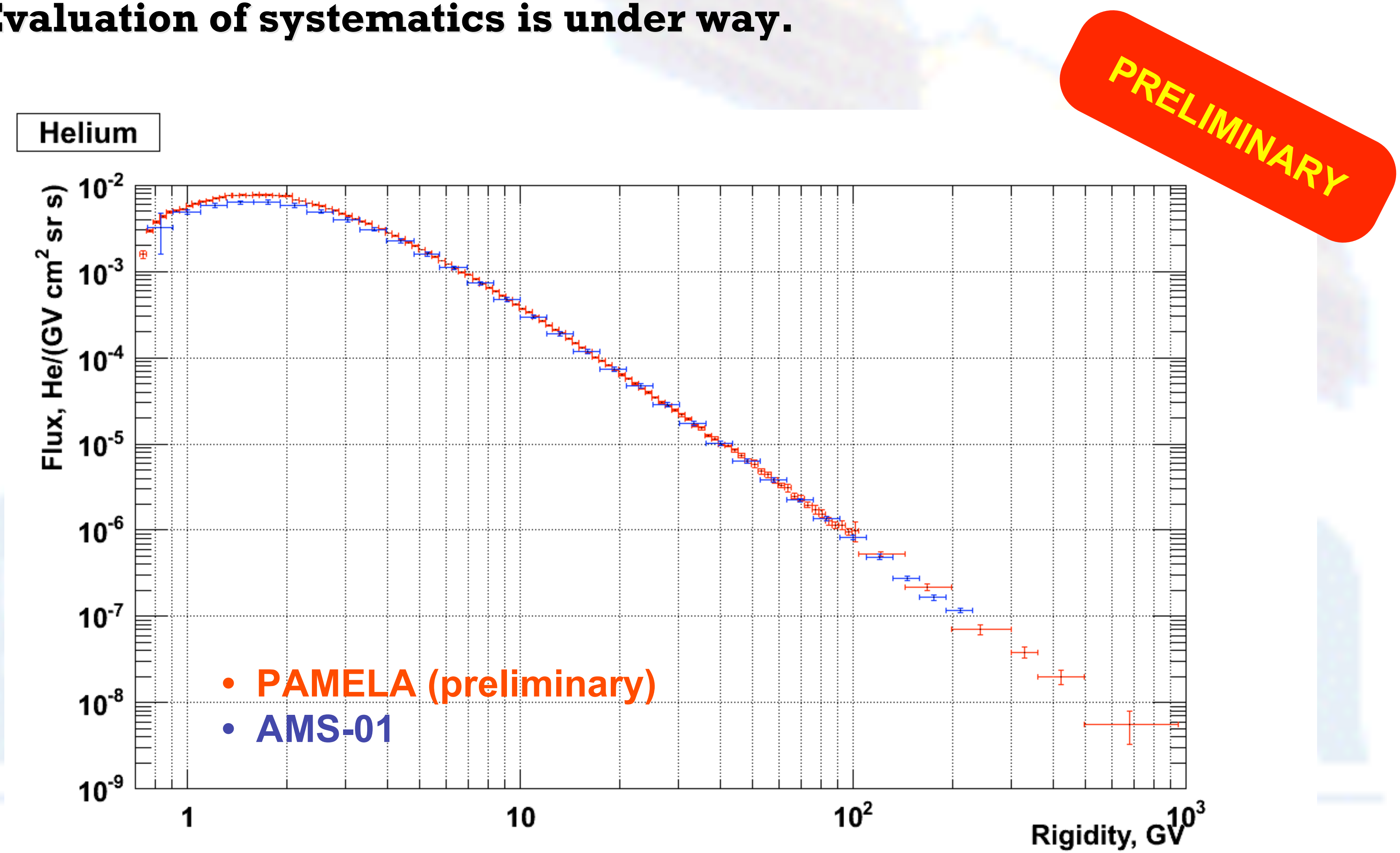

(3.d) Electron absolute flux

Electron selection

- **Two different approaches under development.**

- **(Approach 1) Strong TRK cuts to select negative charges, loose CALO cuts.**
  - **Advantage: CALO selection efficiency is high and ~ constant with energy.**
  - **Disadvantage: main background from spillover protons, limits energy range to ~ 200 GeV (same mechanism seen for the positron fraction).**

- **(Approach 2) Strong CALO cuts to reject hadrons, loose TRK cuts.**
  - **Advantage: energy range can be extended up to ~ 400 GeV.**
  - **Disadvantage: efficiency depends on energy and must be measured with simulation.**

- **Both approaches are currently under finalization.**

Conclusions

- **PAMELA has precisely measured and published both p-bar/p ratio and of positron fraction over a wide energy range.**
  - **Further analysis with new collected statistics is under way, extending energy ranges to the design limits.**
- **Measurements of absolute differential fluxes of several particle species are currently being finalized.**
- **PAMELA is expected to collect data until at least June 2011.**
- **Several other items are currently under study:**
  - **light nuclei (up to Z = 8);**
  - **spectra of high-energy Solar Energetic Particles (SEP);**
  - **radiation belts: morphology and energy spectrum;**
  - **search for anti-He;**
  - **study of isotope composition (d, ^{3}He).**